International Geology Review
2011, iFirst article, 1–32

Elemental mobility in subduction metamorphism: insight from metamorphic rocks of the Franciscan Complex and the Feather River ultramafic belt, California

Arundhuti Ghatak[a,†], Asish R. Basu[a,*] and John Wakabayashi[b]

[a]*Department of Earth and Environmental Sciences, University of Rochester, Rochester, NY 14627, USA;*
[b]*Department of Earth and Environmental Sciences, California State University, Fresno, CA 93740, USA*

(*Acceepted 23 February 2011*)

The degree of element mobility in subduction metamorphism has generated much debate; some workers advocate considerable mobility during metamorphism, whereas others postulate minimal mobility. We assess this issue by examination of major and trace element concentrations and Pb-, Nd-isotopic data for 39 mafic metavolcanic rocks from the Franciscan subduction complex, related units of coastal California, and the Feather River ultramafic belt of the northern Sierra Nevada, California; these samples span a wide range of metamorphic grade. We conclude that these rocks, despite their metamorphism up to eclogite facies, preserve protolith major and trace elemental compositions and isotopic ratios, with the exception of some mobile large ion lithophile elements such as Ba, Pb, and to a smaller extent La, U, and Sr. Thus subduction metamorphism of these metabasalts occurred in a largely closed system. Lack of light rare earth element enrichment in the rocks demonstrates lack of chemical exchange with subducted metasediments. Relatively low SiO_2 content (<48 wt.%) of many of the metamorphic rocks and the lack of correspondence between silica depletion and metamorphic grade suggests that the silica depletion resulted from seafloor hydrothermal alteration before subduction. In spite of demonstrated mobility of Pb, and possible mobility of Nd, isotopic ratios of Pb and Nd were not modified during subduction metamorphism. In contrast to our results from metabasaltic rocks, our analysis of actinolite-rich rinds from high-grade Franciscan mélange blocks suggests some chemical exchange between metachert and the overlying mantle. The increasing enrichment in Ba and Pb with increasing metamorphic grade suggests that Ba- and Pb-rich fluids interacted more intensely with metabasalt at the higher grades of metamorphism. Comparison of these results with studies of the active Mariana forearc suggests that fluids interacting with the mantle wedge up-dip of the region of magma genesis are derived from subducting sediments overlying the down-going plate.

Keywords: element mobility in subduction metamorphism; major and trace elements; Nd, Sr, and Pb isotopes; Franciscan subduction complex; high-grade metamorphism; Feather River ultramafic belt

Introduction

Subduction zones represent avenues of recycling of crustal, atmospheric, and oceanic components to the mantle; metamorphism in the forearc and sub-arc regions of subduction zones likely dictates the extent to which elements are retained in the subducted rocks into the deep mantle or participate in shallower fluid- and melt-related processes such as arc (also known as supra-subduction zone or SSZ) magmatism (Stern and Bloomer 1992). Transfer of mobile elements and volatiles from the slab by dehydration, decarbonation, and melting or assimilation of subducted mafic and sedimentary rocks has been discussed in many studies (e.g. Magaritz and Taylor 1976; Taylor 1986; Pearson *et al*. 1991; Woodhead *et al*. 1993). Most researchers agree that significant transfer of elements from slab to mantle occurs in a subduction-zone setting at the depth of arc magma generation (e.g. Kay 1978; Pearce *et al*. 1992; Tatsumi and Eggins 1995; Yogodzinski *et al*. 1995). In contrast, the degree of element mobility in the subducted slab above the depth of arc magma genesis and the degree to which metamorphic fluids in this regime move up-dip or transfer elements into the overlying mantle are controversial. Some studies have concluded large-scale fluid mobility within the subducting slab with increasing mobility of multiple elements with increasing metamorphic grade (Bebout and Barton 1993; Bebout *et al*. 1993; Bebout 1995; Arculus *et al*. 1999; Becker *et al*. 2000; Bebout 2007), whereas others advocate minimal fluid mobility, even at sample scale (Matthews and Schliestaedt 1984; Barnicoat and Cartwright 1995; Philippot *et al*. 1998; Scambelluri and Philippot 2001; Scambelluri *et al*. 2004; Spandler *et al*. 2004).

Here we report the major and trace element compositions and Nd- and Pb-isotopic ratios of 31 Jurassic to

*Corresponding author. Email: asish.basu@rochester.edu
†Present address: Department of Earth and Environmental Sciences, IISER Bhopal, ITI Campus, Gas Rahat Building, Govindpura, Bhopal-23, Madhya Pradesh, India.

ISSN: 0020-6814 print/ISSN: 1938-2839 online

DOI: 10.1080/00206814.2011.567087
http://www.informaworld.com

Cretaceous-age metavolcanic rocks from the Franciscan Complex (Figure 1), including prehnite-pumpellyite, blueschist, eclogite, and amphibolite-grade rocks, two Coast Range ophiolite (CRO) basalts that have undergone only seafloor hydrothermal metamorphism, three actinolite–chlorite rinds from the Franciscan high-grade blocks (Figure 1, Saha *et al*. 2005), and three amphibolites associated with the metamorphic sole of the Feather River ultramafic belt (FRB) of the northern Sierra Nevada, California, which marks an older (Palaeozoic to early Mesozoic) subduction suture (Smart and Wakabayashi 2009). For comparison, we have also included data from Franciscan metavolcanic rocks analysed in our previous studies (Saha *et al*. 2005; Wakabayashi *et al*. 2010).

In this study we evaluate chemical variability related to original protolith composition and metamorphism. In our previous studies (Saha *et al*. 2005; Wakabayashi *et al*. 2010), we have proposed that the high-grade, earliest subducted rocks of the Franciscan subduction complex have a nascent arc protolith whereas later subducted, low-grade rocks display a MORB parentage. The fact that our high-grade samples from a wide geographical area in the Franciscan are almost identical in trace elements, major elements, and Nd–Pb isotope systematics indicates a

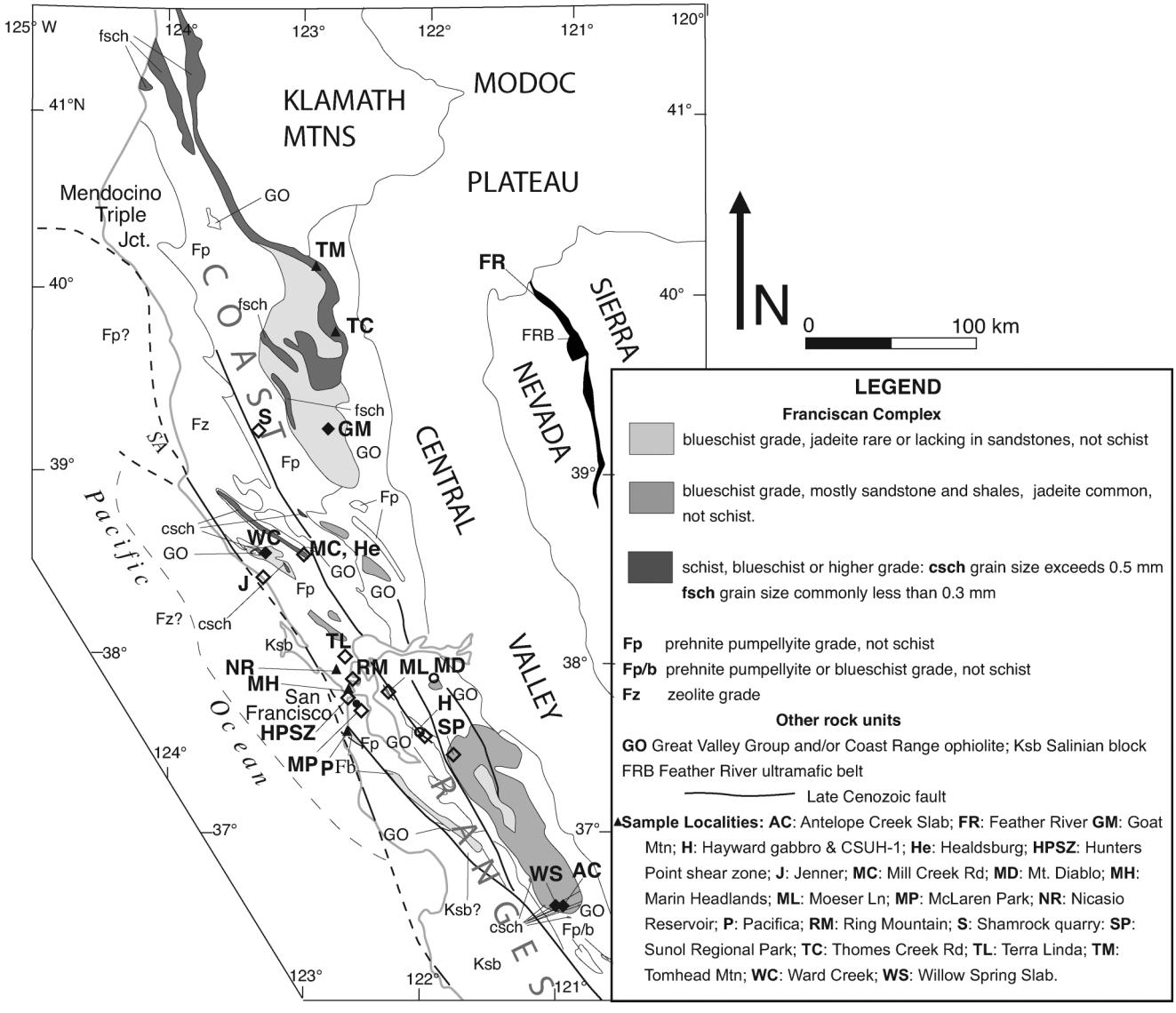

Figure 1. (A) Distribution of Franciscan and related rocks of central and northern California, modified from Wakabayashi *et al.* (2010). Sample field relations and tectonic affinity are denoted by high-grade coherent sheets (filled diamonds), high-grade tectonic blocks (open diamonds), low-grade coherent sheets (filled triangles), and Coast Range ophiolite (open circles). (B) Feather River ultramafic belt (FRB) in the Sierra Nevada, modified from Smart and Wakabayashi (2009). CC, Calaveras Complex; DGO, Devil's Gate ophiolite; RAS, Red Ant Schist; SFU, Shoo Fly Complex; WU, undifferentiated metamorphic and plutonic rocks.

similarity in the geochemical processes during Franciscan subduction. The three high-grade rocks of the FRB used in this study show MORB-like major element composition (Smart and Wakabayashi 2009) and their trace element and isotopic data are also consistent with MORB parentage.

We compare geochemically low- and high-grade MORBs and high-grade arc protolith rocks to assess the mobility of various elements during subduction. This comparison is crucial in evaluating the differences in the behaviour of various major and trace elements and understanding the elemental mobility in a closed system (wherein the original protolith composition is preserved) versus an open system behaviour during the subduction of oceanic crust and subsequent exhumation of these rocks. We show that element mobility is limited in subduction metamorphism of the basaltic slab with the exception of a few elements such as Ba and Pb, but that some chemical exchange did occur between subducted metachert and the overlying mantle.

Geological setting

The Franciscan subduction complex

Here we review the general field relationships and history of the Franciscan Complex to assess how rocks evolved in the subduction complex at any given time due to interaction with metamorphic fluids. The Franciscan Complex of California may be the world's best known subduction complex. It is well known for its subduction-zone metamorphism, particularly high-pressure (HP)/low-temperature (high P/T) metamorphism (Ernst 1970, 1971), and mélange (Hsü). At least 25% of the rocks have undergone high P/T blueschist or higher grade metamorphism (Wakabayashi 1999). The Franciscan Complex formed during continuous east-dipping subduction from >160 Ma to less than 20 Ma (Wakabayashi 1992; Wakabayashi and Dumitru 2007).

The CRO structurally overlies the Franciscan Complex and consists of serpentinized ultramafic rocks, gabbros, basalts, and other plutonic and volcanic rocks (Hopson *et al*. 1981). Depositionally overlying the CRO are the well-bedded sandstones and shales of the Great Valley Group (GVG) that are coeval with the clastic sedimentary rocks of the Franciscan (Dickinson 1970). Both the CRO and the GVG lack burial metamorphism, in contrast to the Franciscan (e.g. Platt 1986). The Franciscan, GVG, and the Sierra Nevada batholith (Figure 1A) represent, respectively, the subduction complex, forearc basin deposits, and the magmatic arc of an ancient arc-trench system (Dickinson 1970).

Franciscan lithologies are primarily clastic (mostly sandstones and shales) with subordinate basaltic volcanic rocks, chert, and minor limestone (Bailey *et al*. 1964; Blake *et al*. 1988). The clastic rocks are off-scraped and under-plated trench sediments (Dickinson 1970). The pelagic and volcanic rocks represent fragments of seamounts, other oceanic rises, and the pelagic cover and upper part of the subducted oceanic crust (Hamilton 1969; MacPherson 1983; Shervais 1990), with some olistostrome blocks from the upper plate (MacPherson *et al*. 1990; Erickson *et al*. 2004).

Franciscan rocks comprise 'coherent' mappable sheets or mélange units that consist of a sheared matrix with included blocks (Blake *et al*. 1988; Wakabayashi 1992; 1999). High-grade metamorphic rocks include blocks-in mélange (referred to as 'high-grade tectonic blocks') and their rare coherent equivalents (referred to as high-grade coherent sheets) and include coarse-grained blueschists (commonly with eclogite or amphibolite precursors), eclogites, amphibolites, and garnet amphibolites (Wakabayashi and Dumitru 2007). Coherent rocks range from zeolite facies to blueschist–greenschist transition grade (Blake *et al*. 1988) with the exception of rare coherent high-grade slabs. High-grade rocks are entirely metabasites with minor metacherts, whereas lower grade coherent metamorphic rocks are mostly metagreywacke and metashales, with lesser proportions of metabasites and metacherts (Coleman and Lanphere 1971; Blake *et al*. 1988). Collectively the high-grade metamorphic rocks make up far less than 1% of Franciscan metamorphic rocks but they are very widely distributed, cropping out at hundreds of localities along the length of the subduction complex (Coleman and Lanphere 1971). Wakabayashi *et al.* (2010) included coherent metabasites of Ward Creek and the structurally lower parts of the Willow Spring Slab, in their 'high-grade' category, although the grade of metamorphism (epidote blueschist) was the same as that of the highest grade 'low-grade' rocks. This distinction was made on the basis of an older metamorphic age and their geochemical characteristics. We will follow this nomenclature in this article.

The age of high-temperature metamorphism in the high-grade rocks is slightly younger than the 165–172 Ma crystallization age of most of the CRO (Shervais *et al*. 2005; Hopson *et al*. 2008). The high-grade blocks yield the oldest metamorphic ages, with Ar/Ar hornblende ages of 157–168 million years (Ross and Sharp 1986, 1988; Wakabayashi and Dumitru 2007; Shervais *et al*. 2011), Lu–Hf garnet ages of 153–169 million years (Anczkiewicz *et al*. 2004), and lower temperature metamorphic or cooling ages ($^{40}Ar/^{39}Ar$ or K/Ar white mica) of 138–159 million years (Wakabayashi and Deino 1989; Wakabayashi and Dumitru 2007). Low-grade coherent blueschist metamorphic ages range from about 130 million years to 80 million years (Wakabayashi 1999; Wakabayashi and Dumitru 2007; Dumitru *et al*. 2010).

High-grade metamorphism evolved along an anticlockwise P–T–time path (P on the positive *y*-axis), (Wakabayashi 1990; Krogh *et al*. 1994; Tsujimori *et al*.

2006a; Page *et al*. 2007), with peak metamorphism temperatures of about 600–850°C (Wakabayashi 1987; 1990; Tsujimori *et al*. 2006b; Page *et al*. 2007) and peak pressures of about 0.5 GPa for the lowest P amphibolites (Wakabayashi 1990) to 2.0–2.5 GPa for eclogites (Tsujimori *et al*. 2006a; Page *et al*. 2007). The lowest grade (mostly epidote blueschist) of the high-grade rocks was accreted after the higher temperature rocks and metamorphosed at about 300–460°C at pressures of 0.8 GPa to as high as 2.2 GPa (Maruyama and Liou 1988; Shibakusa and Maekawa 1997; Tsujimori *et al*. 2006b) at 154 Ma or perhaps earlier (Wakabayashi and Dumitru 2007). Metamorphism in lower grade metamorphic rocks took place under a mildly clockwise or hairpin P–T–time trajectory (Maruyama *et al*. 1985; Maruyama and Liou 1988) at relatively lower temperatures of 300–350°C for epidote blueschists (Blake *et al*. 1988) at 120 Ma (Wakabayashi and Dumitru 2007; Dumitru *et al*. 2010) to 150–250°C for lawsonite blueschist facies rocks (Ernst 1971; Maruyama *et al*. 1985) at 80–120 Ma (Wakabayashi and Dumitru 2007) and ultimately to zeolite and prehnite-pumpellyite temperatures of $<$200°C (Blake *et al*. 1988) for the last 95 Ma. The lower grade blueschist facies rocks formed at pressures of about 0.6 GPa to $>$1.0 GPa (Brown and Ghent 1983; Maruyama *et al*. 1985; Ernst 1993), whereas sub-blueschist grade rocks were metamorphosed at pressures at 0.4 GPa or less (Blake *et al*. 1988). Metamorphic ages of Franciscan rocks approximate the time of subduction because exhumation of these rocks occurred without thermal overprint while subduction and refrigeration were ongoing (Ernst 1988).

Based on their old age, lithology, PT conditions of high-temperature metamorphism, 'anticlockwise' P–T–time paths, and the closeness in age between their high-temperature metamorphism and formational age of the structurally overlying CRO, the high-grade rocks have been suggested to be remnants of a metamorphic sole formed at the inception of subduction beneath hot sub-oceanic upper mantle material (Wakabayashi 1990; Wakabayashi *et al*. 2010). Lower grade and younger Franciscan rocks formed during subsequent subduction accretion (Wakabayashi 1990). The forearc-trench system may not have received continentally derived sediment until ~145 Ma, about 20 Ma after subduction initiated, based on the age of the basal GVG (Surpless *et al*. 2006) and detrital zircon ages from the oldest Franciscan metaclastic unit, the Skaggs Springs schist (Snow *et al*. 2010). Voluminous accretion of Franciscan metaclastic rocks did not begin until about 120 Ma (Dumitru *et al*. 2010).

Previous geochemical studies of low-grade coherent Franciscan volcanic rocks suggest that these rocks are MORB and ocean island basalts (OIB) (Shervais and Kimbrough 1987; MacPherson *et al*. 1990; Shervais 1990; Wakabayashi *et al*. 2010). Meta-igneous mélange blocks (fine-grained blueschist and lower grade rocks) include those of OIB, MORB, as well as island-arc geochemical signatures (MacPherson *et al*. 1990).

Most coherent volcanic rocks within the Franciscan have estimated formational ages that are much older than the age at which they were subducted, indicating that the ocean crust from which they were derived was old at the time of its arrival at the Franciscan trench, and had travelled thousands of kilometres from its site of formation to the trench (Wakabayashi 1999; Dumitru *et al*. 2010; Wakabayashi *et al*. 2010). In contrast to the coherent volcanic rocks in the Franciscan Complex, most of the CRO volcanic rocks exhibit island-arc chemistry and are thought to represent the early stages of arc development (Giaramita *et al*. 1998; Shervais 2001). Some of the CRO volcanic rocks and dikes exhibit MORB chemistry (Giaramita *et al*. 1998; Shervais 2001), and these have been interpreted as rocks that postdate the main stage of formation of the ophiolite and are the products of subsequent ridge subduction beneath the ophiolite (Shervais 2001). Major, trace elements, and Nd, Sr, and Pb isotopes from Franciscan high-grade rocks indicate nascent island-arc basalt protoliths and these data were interpreted to support a model in which the CRO and Franciscan high-grade metabasite protoliths formed at the same spreading system (Saha *et al*. 2005; Wakabayashi *et al*. 2010).

Feather River ultramafic belt

The 150 km-long, 1–8 km-wide FRB of the northern Sierra Nevada, California (Figure 1B), comprises variably serpentinized ultramafic rocks, with lesser amounts of metagabbro, metadiabase, and metabasalt; collectively these rocks have been considered an ophiolite (Ehrenberg 1975; Sharp 1988; Edelman and Sharp 1989; Edelman *et al*. 1989; Saleeby *et al*. 1989). All rocks of the FRB have undergone metamorphism at amphibolite grade, although there are significant internal differences in metamorphic conditions, with a particularly wide range in metamorphic pressure (Smart and Wakabayashi 2009). The FRB has yielded a large range in igneous (385 ± 10 million years and $314 + 10/-8$ million years, Saleeby *et al*. 1989) and metamorphic ages (about 234–387 million years, Ar/Ar and K/Ar; Weisenberg and Avéallemant 1977; Hietanen 1981; Böhlke and McKee 1984) and it has been called a polygenetic ophiolite (Saleeby *et al*. 1989). These rocks represent the record of a much older ocean basin-subduction system than that preserved in the CRO–Franciscan pair.

Directly west of the ultramafic contact in the North Fork Feather River area is a $<$300 m-thick unit of amphibolite facies metamorphic rocks, the external schist of Ehrenberg (1975). Williams and Smyth (1973) and Ehrenberg (1975) suggested that the external schist may represent a metamorphic sole. The structures (high-temperature ultramafic side-up shear sense), structural position beneath ultramafic rocks, oceanic lithologies (primarily metabasalt,

with subordinate metachert and metaclastic rocks), and high-temperature, HP metamorphism (≥750°C, 13–19 kb for the highest grade rocks) also confirm a metamorphic sole origin for these rocks (Smart and Wakabayashi 2009). A date of 236 ± 4 Ma (Ar/Ar, hornblende; Weisenberg and Avéallemant 1977) from a lens of HP amphibolite within ultramafic rocks may date the HP, high-temperature metamorphism in the external schists. The presence of low-pressure (≤0.5 GPa) amphibolites associated with the FRB indicates significant exhumation of the external schists (metamorphic sole) relative to some parts of the FRB; this exhumation occurred prior to 177 Ma based on the presence of breccia clasts composed of external schist found in the Calaveras Complex, a unit that is present west of, and adjacent to, the external schist (Smart and Wakabayashi 2009).

Collectively the existing structural and metamorphic relationships indicate that the external schist of the FRB represents a metamorphic sole that formed at the inception of intra-oceanic subduction, analogous to the highest grade rocks of the Franciscan, as well as worldwide occurrences of metamorphic soles. The principal differences between the external schist and the Franciscan high-grade rocks are the occurrence of rock of MORB as well as SSZ origin in the FRB external schist versus entirely SSZ origins for samples collected from the Franciscan high-grade rocks, and the occurrence of high-grade metaclastic rocks in the FRB external schist. These two groups of rocks of different protolith compositions were chosen to study elemental mobility during subduction, as discussed below.

Samples analysed and analytical methods

For this study, major and trace element concentrations and high precision Nd- and Pb-isotopic ratios of 34 Franciscan samples, two CRO samples, and three FRB amphibolites were analysed. These samples (Table 1) include rocks from high-grade blocks (Hayward, Moeser Lane, Mill Creek Road, Jenner, Shamrock Quarry, Terra Linda, Hunter's Point, Sunol, Healdsburg), high-grade coherent sheets (Willow Spring Slab and the Antelope Creek Slab of the Panoche Pass area, Goat Mountain, Ward Creek), low-grade coherent sheets (Nicasio Reservoir, Marin Headlands, Pacifica, Thomes Creek Road, and Tomhead Mountain), CRO basalts (Mt Diablo) and CRO gabbro (Hayward) (Figure 1A), and amphibolites from the FRB (Figure 1B).

Whole-rock samples were powdered using a spex alumina ball mill at the University of Rochester. Starting with 1 kg size rock sample, we broke them into chips which we washed and dried, and finally selected 10 g of these chips to be powdered for each sample to ensure that the powder was representative of the whole-rock sample. Thin sections were prepared and examined for each of these rocks for determination of mineralogy (Appendix).

A commercial laboratory was used for the analysis of major elements (Activation Laboratories Ltd., Ancaster, Ontario, Canada). These analyses are certified to be within 2% of known rock standards. All the other trace element and isotopic analyses reported here were carried out at the University of Rochester.

Trace element concentrations were measured using an Inductively Coupled Plasma Mass Spectrometer (Thermo Elemental X-7 series) at the University of Rochester. Twenty-five milligramme powdered rock samples were digested using $HF–HNO_3$ acid mixtures and diluted to a 100 ml solution with 2% HNO_3. Each sample was then spiked with a 10 ppb internal standard of In, Cs, Re, and Bi. BCR-2 (basalt-USGS) was used as a known external standard while AGV-2 (andesite-USGS) and BHVO-2 (basalt-USGS) rock standards were run as unknowns to estimate external error in the trace element analyses reported here (Table 3). Analytical uncertainties are usually less than 5% for most of the trace elements and commonly less than 2% for the rare earth elements (REEs).

Nd- and Pb-isotopic ratios were measured with a multi-collector Thermal Ionization Mass Spectrometer (VG Sector at the University of Rochester) for which 100–200 mg powdered rock samples were dissolved in $HF–HNO_3$ and HCl acids. Nd and Sr isotopes were measured using the procedures established for our laboratory at the University of Rochester (Basu *et al*. 1990). Measured $^{143}Nd/^{144}Nd$ ratios were normalized to $^{146}Nd/^{144}Nd = 0.7219$. Uncertainties for the measured $^{143}Nd/^{144}Nd$ ratios were less than +0.00003. La Jolla Nd standard analysed during the course of this study yielded $^{143}Nd/^{144}Nd = 0.511856 \pm 0.000024$ (2σ) ($n = 4$). Initial ε_{Nd} values were calculated using present-day bulk earth $^{143}Nd/^{144}Nd$ of 0.512638 and $^{147}Sm/^{144}Nd$ of 0.1968 (Jacobsen and Wasserburg 1984). Pb isotopes were also measured in our laboratory in Rochester using the silica-gel technique established previously (Sharma *et al*. 1992). Filament temperature during Pb-isotopic ratio measurements was monitored continuously and raw ratios were calculated as weighted averages of the ratios measured at 1150°C, 1200°C, and 1250°C, respectively. The reported Pb-isotopic data were corrected for mass fractionation of 0.12 ± 0.03% per a.m.u. based on replicate analyses of the NBS-981 Equal Atom Pb standard measured in the same fashion. Estimated errors are less than 0.05% per mass unit. Our laboratory procedural blanks were less than 200 pg for both Nd and Pb. No blank correction was necessary for the isotopic ratios.

Geochemical results

Major elements

Major element data for 34 Franciscan and 2 CRO samples of our study are given in Table 2. We present the major element data mainly as a starting point for the general discussion of whole-rock chemistry of these rocks.

Table 1. Rock names, localities, and tectonic affinities of the 34 Franciscan, 2 Coast Range ophiolite, and 3 Feather River ultramafic belt samples of this study. Sample localities are also shown in Figure 1.

Tectonic affinity, category	Sample number	Rock type	Locality
Franciscan high-grade coherent	GM-1	Garnet amphibolite	Goat Mountain
	GM-2	Garnet amphibolite	
	GM-3	Garnet amphibolite	
	F-3	Garnet amphibolite	Antelope Creek Slab
	WC-SSS-1	Epidote blueschist	Ward Creek
	WC-MV-1	Epidote blueschist	
	WC-MV-2	Epidote blueschist	
	95-DIAB-14	Epidote blueschist	Willow Spring Slab
	95-DIAB-29	Epidote blueschist	
	95-DIAB-031	Eclogite	
	95-DIAB-107C	Eclogite	
Franciscan high-grade tectonic block	CSUH-1	Amphibolite	Hayward
	SUNOL-2038	Eclogite	Sunol
	JS-Ecg	Eclogite	Healdsburg
	HPSZ	Garnet amphibolite	Hunter's Point
	F-1	Garnet amphibolite	Moeser Lane
	F-4	Eclogite	Jenner
	F-6	Garnet amphibolite	Shamrock Quarry
	F-8	Eclogite	Jenner
	F-10	Epidote blueschist	Mill Creek Road
	F-11	Eclogite	Mill Creek Road
	MP-1	Amphibolite	McLaren Park
	TL-4	Amphibolite	Terra Linda
Franciscan low-grade coherent	NR-GABB	Gabbro, prehnite-pumpellyite facies	Nicasio Reservoir
	NR-PB	Pillow basalt, prehnite-pumpellyite facies	Nicasio Reservoir
	MHPB	Pillow basalt, prehnite-pumpellyite facies	Marin Headlands
	PAC-1	Basalt, prehnite-pumpellyite facies	Pacifica
	SFM-1	Epidote blueschist	Tomhead Mountain
	SFM-6	Epidote blueschist	Tomhead Mountain
	F-9	Epidote blueschist	Thomes Creek Road
	F-12	Epidote blueschist	Thomes Creek Road
Tectonic affinity	Sample number	Rock type	Locality
Coast Range ophiolite	MT.DIAB-1	Basalt	Mt Diablo
	HW-GABB	Gabbro	Hayward
Feather River ultramafic belt	YR 44	Amphibolite	North Fork Feather River
	YR 45	Amphibolite	North Fork Feather River
	FR 92-4	Garnet amphibolite	North Fork Feather River
Franciscan high-grade block rinds	GT/GL (1)	Actinolite rind	Ring Mountain
	R/GT	Actinolite rind	Ring Mountain
	TIBB-R	Actinolite rind	Ring Mountain

In the total alkali versus silica variation diagram (Figure 2), SiO_2 contents of the high-grade rocks show a range from 43% to 54%, and the (Na_2O+K_2O) contents vary from 3% to 7%, indicating a calc-alkaline trend similar to those in orogenic belts. The low-grade metavolcanics fall almost entirely in the field of basalts with the lowest (Na_2O+K_2O) and SiO_2 contents. The majority of the samples have SiO_2 content less than ~48 wt.%, which is usually the minimum for the SiO_2 contents of tholeiitic and calc-alkaline basaltic rocks from different tectonic settings (e.g. Carmichael *et al*. 1974).

Variation of SiO_2 wt.% and K_2O wt.% with increasing metamorphic grades of the Franciscan rocks is shown in Figure 3. The grades of metamorphism range from unmetamorphosed CRO to prehnite-pumpellyite facies rocks,

Table 2. Major element compositions (wt.%) of all the rocks of this study from the Franciscan Complex and CRO.

	GM-1	GM-2	GM-3	F-3	WC-SSS-1	WC-MV-1	WC-MV-2	95-DIAB-14	95-DIAB-29	95-DIAB-031	95-DIAB-107C	
	High-grade Franciscan rocks											
SiO_2	48.5	48.1	44.8	44.5	48.9	47.8	49.4	51.9	43.3	44.7	48.2	
Al_2O_3	15.2	13.8	12.3	13.7	15.8	15.5	15.0	17.7	14.3	14.0	14.5	
Fe_2O_3(T)	10.1	14.3	17.1	16.7	9.8	10.7	10.2	7.6	8.5	13.2	10.6	
MnO	0.20	0.22	0.23	0.38	0.17	0.19	0.19	0.12	0.12	0.30	0.21	
MgO	8.3	8.3	8.4	7.5	8.6	7.3	7.7	6.3	6.3	7.1	7.5	
CaO	8.5	5.3	8.2	9.6	7.1	11.0	9.8	6.5	14.0	11.2	10.4	
Na_2O	3.12	3.34	2.71	2.57	1.48	2.16	3.34	4.33	3.22	4.26	2.67	
K_2O	0.71	0.17	0.40	0.19	1.64	0.85	0.23	0.38	0.77	0.08	1.81	
TiO_2	0.88	1.37	2.41	2.00	1.70	1.23	1.30	0.61	1.04	1.94	1.14	
P_2O_5	0.06	0.11	0.22	0.26	0.17	0.10	0.08	0.05	0.11	0.11	0.10	
LOI	4.55	5.30	3.77	2.34	4.84	3.24	3.11	4.48	8.63	3.13	1.88	
Total	100.2	100.3	100.5	99.8	100.3	100.1	100.3	100.0	100.3	100.0	99.1	

	CSUH-1	SUNOL-2038	JS-Ecg	HPSZ-META	F-1	F-4	F-6	F-8	F-10	F-11	MP-1	TL-4
	High-grade Franciscan rocks											
SiO_2	46.1	44.6	48.4	46.5	53.7	47.6	50.3	46.3	48.4	44.6	50.6	54.2
Al_2O_3	15.3	15.0	6.1	12.4	15.8	12.6	13.2	12.1	11.9	13.4	13.2	11.8
Fe_2O_3(T)	11.6	13.2	13.3	11.7	9.8	16.9	13.4	12.5	11.9	13.1	12.7	8.8
MnO	0.17	0.19	0.20	0.17	0.21	0.25	0.24	0.21	0.16	0.25	0.22	0.16
MgO	7.8	8.8	11.6	6.7	5.5	6.3	7.4	5.5	14.9	7.5	5.6	8.5
CaO	5.8	11.2	12.7	14.1	6.3	7.8	9.1	14.1	1.5	11.3	10.0	9.6
Na_2O	4.82	3.16	2.98	2.75	5.93	3.78	3.20	3.85	4.38	3.98	3.14	4.01
K_2O	2.25	0.50	0.13	0.60	0.27	0.13	0.21	0.40	0.73	0.48	0.41	0.13
TiO_2	1.93	0.69	2.65	1.16	0.88	3.16	1.85	2.78	0.72	1.88	1.32	0.46
P_2O_5	0.14	0.02	0.03	0.11	0.09	0.51	0.24	0.57	0.12	0.14	0.08	0.09
LOI	3.80	2.39	1.62	3.57	1.32	0.94	0.57	0.40	4.54	2.55	2.63	2.25
Total	99.7	99.8	99.7	99.7	99.8	100.0	99.8	98.8	99.1	99.2	100.0	100.1

	NR-GABB	SFM-1	SFM-6	F-9	F-12	MHPB	PAC-1	MT.DIAB-1	HW-GABB	GT/GL (1)	R/GT	TIBB-R
	Franciscan Low-Grade Rocks							Coast Range ophiolites		Rinds		
SiO_2	46.2	38.1	48.8	45.6	47.2	60.8	46.6	48.4	41.3	51	56	46.45
Al_2O_3	16.9	16.2	14.3	13.2	12.3	9.5	13.6	14.2	16.2	8.93	3.02	15.83
Fe_2O_3(T)	9.3	16.7	13.9	13.9	14.2	10.7	11.1	11.3	19.6	7.95	6.21	9.04
MnO	0.16	0.28	0.27	0.23	0.21	0.16	0.12	0.21	0.21	0.21	0.23	0.16
MgO	9.1	5.7	3.6	6.5	6.0	2.8	8.9	4.3	7.5	16.5	19.6	12.9
CaO	7.8	13.6	12.8	10.6	9.9	10.1	8.7	10.0	12.8	8.98	10.6	5.03
Na_2O	2.82	0.53	0.28	2.33	2.85	0.20	1.83	4.72	0.69	2.47	1.43	2.55
K_2O	1.15	0.26	0.06	0.04	0.01	0.01	0.11	0.16	0.03	0.22	0.22	2.58
TiO_2	1.49	2.70	2.37	2.31	2.63	1.76	1.62	2.06	1.10	0.30	0.05	0.45
P_2O_5	0.18	0.21	0.17	0.21	0.24	0.19	0.12	0.13	0.03	0.01	0.01	0.01
LOI	4.99	5.78	3.48	4.48	3.61	3.73	7.38	4.72	0.72	2.04	1.90	3.62
Total	100.2	100.1	99.9	99.5	99.2	99.8	100.2	100.3	100.1	99.9	99.7	99.6

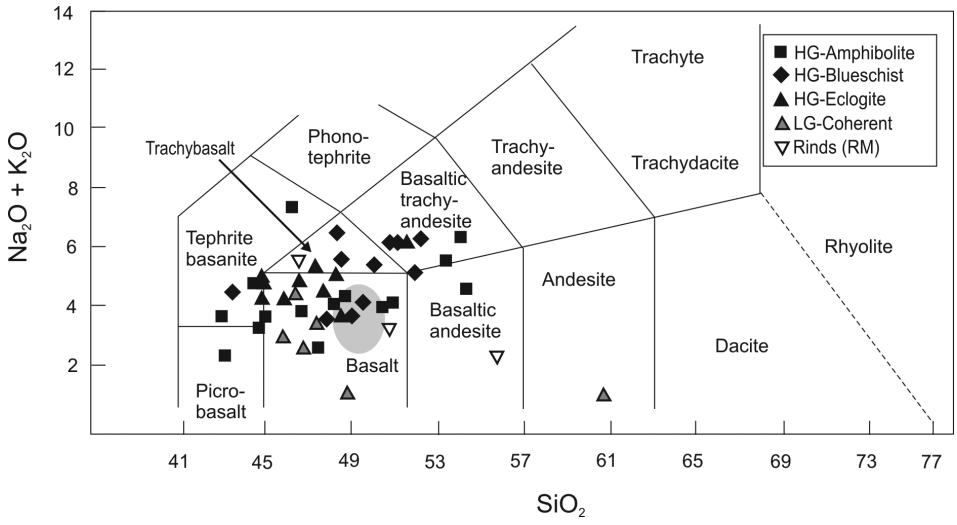

Figure 2. Na_2O and K_2O versus SiO_2 wt.% in whole-rock samples of the Franciscan high- and low-grade metamorphic rocks. These data and data plotted in subsequent figures also include our recently published results of the blueschists, eclogites, and grt-amphibolites (Saha *et al*. 2005; Wakabayashi *et al*. 2010) including actinolite rinds from high-grade blocks from the Ring Mountain (RM) locality. HG, Franciscan high-grade rocks; LG, Franciscan low-grade coherent rocks (Figure 1A).

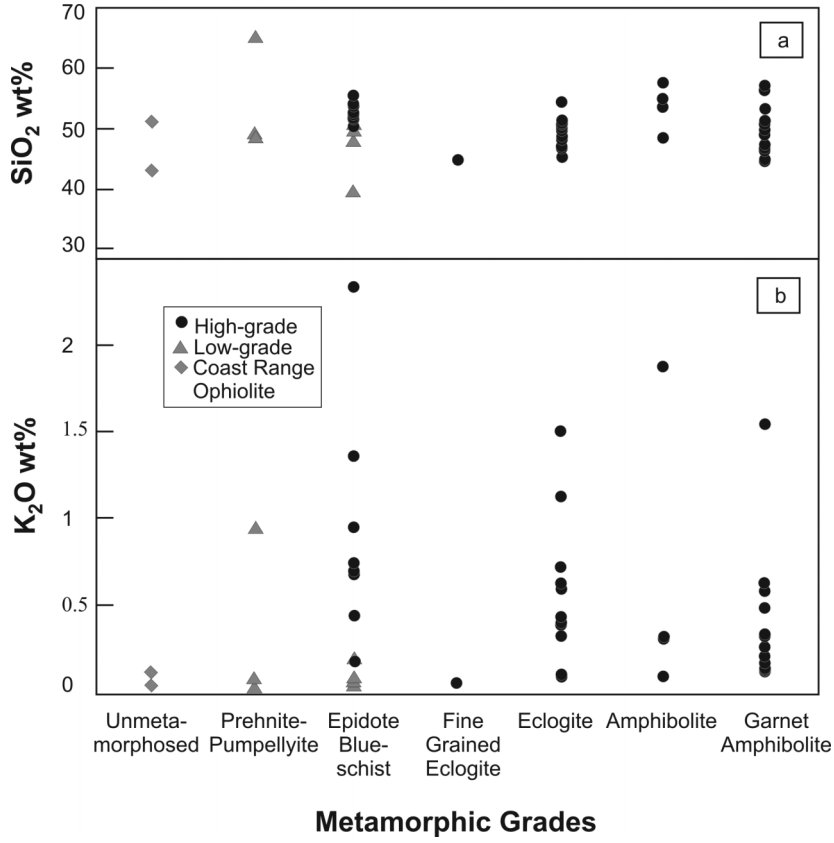

Figure 3. Variation of (A) SiO_2 wt.% and (B) K_2O wt.% with increasing metamorphic grades of the Franciscan Complex rocks. The metamorphic grades are the highest metamorphic conditions the rocks experienced.

epidote blueschist, fine-grained eclogite, eclogite, amphibolite, and garnet amphibolite. A few of the high-grade blueschists were originally eclogite/amphibolites that retrograded to blueschist facies. We have considered the peak metamorphic conditions in our petrographic analysis of metamorphic grades. Note that there is no systematic depletion or enrichment of silica or potassium with increasing grade of metamorphism (Figure 3).

In the bivariant major element variation diagrams, plotted against the SiO_2 contents (Figure 4), the high-grade rocks show a generally positive trend for Na_2O, negative for FeO* (where FeO* is total Fe) and CaO, and relatively flat trends for MgO and P_2O_5. The grey areas contain the bulk-rock analyses of five low-grade rocks of 45–49 wt.% SiO_2 content (Figure 4). We analysed comparatively few low-grade rocks from a wide geographic extent within the Franciscan, and they show a restricted range in their major element variation as compared with the high-grade rocks. Mg # [100 × molar MgO/(MgO+FeO*)], when plotted against FeO* and TiO_2 (Figure 5), shows a distinct negative correlation that is commonly seen in igneous rock suites and may reflect the protolith compositional variations of the high-grade rocks.

Rare earth and other trace elements

Trace element data for all Franciscan, CRO, and Feather River rocks of this study are presented in Table 3. The chondrite-normalized REE patterns for these Franciscan high- and low-grade rocks and the Feather River

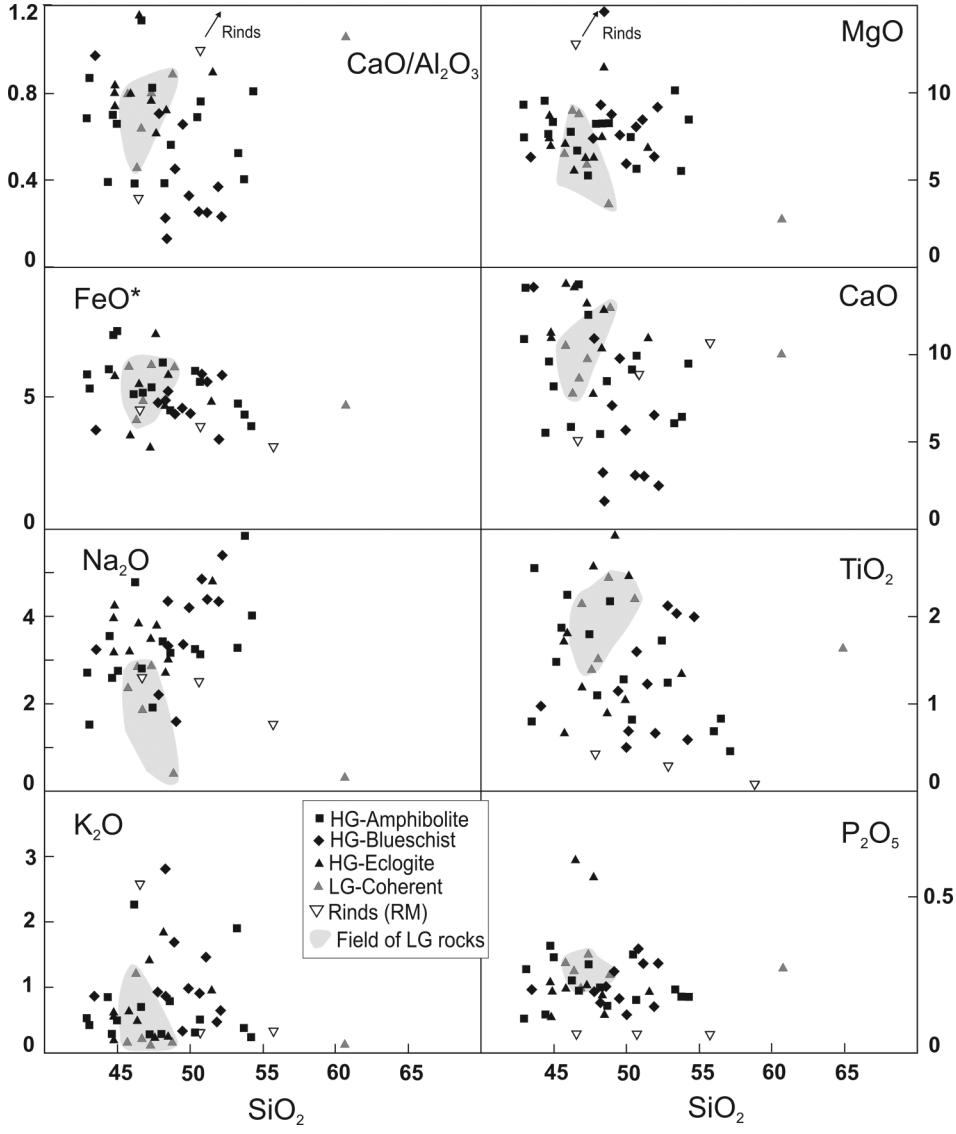

Figure 4. Harker variation diagram for Franciscan Complex rocks of this study and those of our previous studies (Saha *et al*. 2005; Wakabayashi *et al*. 2010). The grey areas in these figures depict the range for the low-grade rocks. HG, Franciscan high-grade rocks; LG, Franciscan low-grade coherent rocks; RM, Ring Mountain locality.

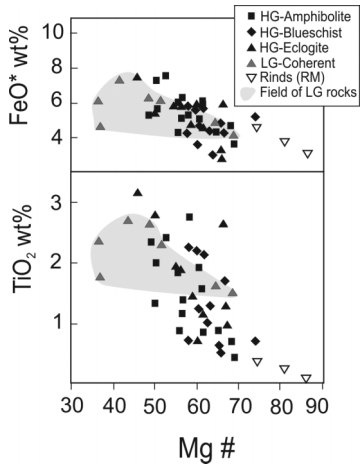

Figure 5. Variation of TiO_2 and FeO* wt.% (FeO* = total Fe as FeO) with Mg # (defined in text) for all the Franciscan rocks of this and our previous studies Wakabayashi *et al.* (2010) and Saha *et al.* (2005). The grey areas are the range of the low-grade coherent rocks. Abbreviations are as in Figure 2.

amphibolites (Figure 6) are compared with Western Pacific arc tholeiite data (Jakes and Gill 1970). The Franciscan high-grade rocks display generally flat REE patterns (Figure 6A). The high-grade Feather River samples show light rare earth element (LREE) depletions similar to N-MORB (Figure 6B). Most of the low-grade coherent rocks of this study also show slight LREE depletions similar to N-MORB. The Pacifica and one of the Nicasio Reservoir samples (Figure 6B) show slight enrichments in LREE (La, Ce, and Pr). In Figure 6B we have plotted for comparison average Post-Archaean Australian Shale (PAAS, Taylor and McLennan 1985) and average Pacific Ocean pelagic sediments (Plank and Langmuir 1998). It is clear from this comparison that the REE plots are strikingly different from PAAS and the pelagic sediments (Figure 6). This difference has important implications for this study and will be discussed in the next section.

Twenty-five compatible and incompatible trace element concentration patterns are shown normalized to N-MORB in Figure 7. High-grade Franciscan rocks (Figure 7A) show relatively high Ba and Pb concentrations and high Ba/Rb, Ba/Th, U/Th, U/Nb, La/Nb ratios. Distinct negative Nb and Ta anomalies are observed in most of these rocks and they show low Ce/Pb ratios. Low-grade rocks and Feather River amphibolites (Figure 7B) lack the high U/Nb ratio and a generally negative Nb–Ta anomaly of the high-grade Franciscan rocks. Ring Mountain rinds (Figure 7B) have low Nb (although Ta is anomalous) and high Ba and Pb.

The ranges of several compatible–incompatible and incompatible–incompatible element ratios, such as $[La/Sm]_N$, Ba/La, Ce/Pb, Th/Nb, La/Nb, and Th/Yb, are shown in Figures 8–10. The trace element data for the high-grade rocks display elevated ratios of fluid-soluble elements, most notably Ba and Pb, and moderately Rb, Sr, and U, compared with fluid-insoluble elements Th, Nb, and Ta. This gives rise to elevated ratios of large ion lithophile elements (LILE) relative to both high field-strength elements and heavy rare earth elements (HREEs).

Variation of Ba/La with increasing values of $[La/Sm]_N$ normalized to chondrite (Figure 8) is useful in determining the degree of sediment input as well as the fluid component in the bulk rocks (Kent and Elliott 2002). In this figure, Franciscan high- and low-grade rocks and Feather River high-grade rocks are compared with the fields of MORB, OIB, altered oceanic crust, and Mariana bulk sediments. The field for the high-grade rocks, extending far from the MORB composition (Figure 8), is consistent with fluid mobility during subduction of these rocks. Feather River and low-grade Franciscan rocks fall entirely within the field of MORB and OIB. There is a notable absence in these rocks of any subducted sediments, such as those similar to the Mariana bulk sediment (Figure 8), which consists of pelagic clay, volcanoclastic turbidites, and chert (Elliott *et al*. 1997).

In a plot of Ce/Pb versus Ce (Figure 9), samples from the current study and our previous studies (Saha *et al*. 2005; Wakabayashi *et al*. 2010) are compared with MORB, OIB, average continental crust, and bulk silicate Earth. Most Franciscan high-grade rocks fall within the field of global arc tholeiites (Figure 9). It is noted that the low-grade rocks are closer to the MORB values whereas the high-grade rocks show a large range in their Ce/Pb ratios and Pb concentrations (Figure 9).

La is plotted against Th with both elements normalized to Nb in Figure 10. In this Th/Nb versus La/Nb plot, all Franciscan and Feather River rocks are compared to fields of MORB and OIB, upper continental crust (UCC), and intra-oceanic arc volcanics (i.e. Izu-Bonin, Mariana, and Kurile arcs). All low-grade Franciscan and high-grade Feather River rocks of this study fall entirely within the field of MORB and OIB, whereas high-grade Franciscan rocks plot within the field of Marianas arc. Note that in Figure 10 both MORB and OIB fields show a narrow range, but they overlap all the intra-oceanic arc volcanics with which our Franciscan geochemical data are being compared.

Radiogenic isotope compositions

Initial $^{206}Pb/^{204}Pb$, $^{207}Pb/^{204}Pb$, and $^{208}Pb/^{204}Pb$ of Franciscan rocks show ranges of 18.13–20.15, 15.49–15.88, and 37.16–39.55, respectively (Table 4). Initial Pb-isotopic ratios for high-grade Franciscan rocks and the CRO have been calculated at 169 million years, the age of crystallization of the CRO (Shervais *et al*. 2005; Hopson *et al*. 2008) and the oldest age of metamorphism of the high-grade rocks (Anczkiewicz *et al*. 2004). For low-grade Franciscan rocks, the initial ages vary from 195 million years to 130 million years (Table 4) based on

Table 3. Trace element compositions of all the high-grade blocks, high-grade coherent sheets, low-grade coherent sheets, and CRO samples of this study from different localities of the Franciscan Complex (Figure 1). Trace element concentrations are in ppm with analytical uncertainties within 5%.

	GM-1	GM-2	GM-3	F-3	WC-SSS-1	WC-MV-1	WC-MV-2	95-DIAB-14	95-DIAB-29	95-DIAB-031	95-DIAB-107C	CSUH-1	SUNOL-2038
							High-grade Franciscan rocks						
Rb	15.9	1.34	4.55	4.21	25.8	20.27	3.68	3.61	14.5	1.38	47.4	64	7.4
Ba	135	242	156	220	90	60	51	30	46	164	240	516	398
Sr	85	76	31.6	68	131	135	201	200	228	788	232	12.5	307
Pb	0.73	0.87	0.06	1.27	0.81	0.60	0.70	1.80	0.69	43.0	9.9	85	4.05
La	2.00	4.08	5.52	7.1	7.4	2.90	2.98	8.7	3.13	8.36	3.32	5.7	1.41
Ce	4.72	10.2	18.0	17.8	19.6	8.9	9.0	19.8	8.6	21.7	8.6	16.9	3.24
Pr	1.00	1.76	3.34	2.68	2.96	1.58	1.59	2.82	1.37	3.42	1.69	2.84	0.52
Nd	5.7	9.1	15.0	13.4	11.4	8.5	8.5	12.4	5.6	13.5	9.2	14.7	2.65
Sm	2.25	3.30	7.01	4.50	4.13	3.07	3.04	3.27	2.23	5.2	4.07	5.93	1.06
Eu	0.98	1.31	2.21	1.54	1.5	1.22	1.15	1.05	0.86	1.94	1.62	2.03	0.44
Gd	3.44	4.72	10.1	6.2	5.2	4.24	4.16	3.53	3.07	6.7	5.4	6.2	1.09
Tb	0.63	0.85	1.84	1.13	0.85	0.77	0.75	0.55	0.52	1.18	1.00	1.08	0.19
Dy	4.18	5.6	11.8	7.6	5.4	4.96	4.81	3.31	3.48	7.4	6.3	6.8	1.21
Ho	0.95	1.22	2.67	1.77	1.15	1.09	1.06	0.71	0.74	1.63	1.32	1.47	0.27
Er	2.71	3.48	7.5	5.4	3.15	3.02	3.00	1.97	2.03	4.52	3.52	4.08	0.79
Tm	0.41	0.53	1.14	0.87	0.46	0.44	0.45	0.29	0.30	0.65	0.50	0.59	0.12
Yb	2.61	3.42	7.7	5.9	2.78	2.82	2.88	1.80	1.88	4.20	3.07	3.68	0.86
Lu	0.39	0.51	1.18	0.91	0.39	0.39	0.42	0.25	0.27	0.62	0.44	0.47	0.13
Y	27.1	32.7	76.9	52	32.1	29.5	28.1	17.5	21.7	44.6	37.1	39.7	7.4
Th	0.12	0.43	0.54	0.64	0.53	0.20	0.18	1.42	0.21	0.73	0.37	0.30	0.23
U	0.21	0.25	0.43	0.16	0.17	0.18	0.10	0.42	0.16	0.38	0.39	0.32	0.47
Zr	10.7	14.4	24.7	19.5	2.08	4.11	2.59	7.3	2.74	6.8	3.04	28.1	4.74
Hf	0.61	0.86	1.24	0.95	0.15	0.33	0.20	0.25	0.11	0.30	0.21	1.19	0.24
Nb	1.07	3.64	12.4	10.7	8.5	2.35	2.51	1.82	3.66	10.0	1.85	4.84	0.73
Ta	0.05	0.20	0.70	0.65	0.47	0.13	0.14	0.14	0.26	0.58	0.08	0.31	0.02
Sc	44.0	58.8	58.7	51	41	43.0	45.1	26.8	31.4	53.2	50.5	43.9	47.8
V	257	402	524	456	286	287	293	1228	172	466	368	347	468

Table 3. (Continued).

	JS-Ecg	HPSZ-META	F-1	F-4	F-6	F-8	F-10	F-11	MP-1	TL-4	NR-GABB	NRPB	MHPB	PAC-1
					High-Grade Franciscan Rocks						Franciscan Low-Grade Rocks			
Rb	0.13	7.3	2.41	2.65	2.49	11.3	15.1	11.9	10.8	0.59	0.23	17.6	0.01	1.51
Ba	5.0	113	186	40	28	225	495	686	140	19.9	76	156	87	24
Sr	76	60	155	99	93	308	8	612	67	17.2	288	450	26	70
Pb	2.03	0.79	2.26	2.78	1.09	4.23	1.02	9.2	0.66	0.66	4.48	0.67	6.9	0.99
La	10.6	2.58	4.68	9.2	3.96	8.0	5.0	5.7	2.89	3.52	20.3	8.3	5.8	5.6
Ce	32.4	6.6	10.7	27.1	12.6	24.3	10.8	15.8	6.5	8.2	39.6	18.5	15.9	14.9
Pr	4.35	1.22	1.60	4.44	2.22	4.24	1.67	2.77	1.39	1.24	5.5	2.43	2.65	2.27
Nd	20.6	6.4	7.6	22.8	12.1	22.9	7.8	14.4	6.3	5.9	23.7	8.4	13.7	10.9
Sm	5.4	2.39	2.34	8.1	4.56	8.4	2.55	4.97	3.03	1.64	6.0	2.69	4.54	3.25
Eu	1.53	0.83	0.72	2.60	1.55	2.94	0.83	1.69	1.24	0.58	2.09	1.12	1.48	1.19
Gd	5.5	3.48	2.96	10.6	6.3	11.8	3.32	6.7	4.74	1.92	7.2	3.00	6.3	3.96
Tb	0.72	0.64	0.52	1.88	1.13	2.03	0.58	1.19	0.84	0.31	1.20	0.50	1.11	0.65
Dy	3.78	4.39	3.32	11.4	7.4	11.7	3.63	7.5	5.5	1.96	7.4	3.06	7.2	3.97
Ho	0.75	0.99	0.72	2.35	1.67	2.43	0.80	1.64	1.24	0.41	1.58	0.65	1.61	0.81
Er	1.98	2.97	1.98	6.3	4.82	6.7	2.32	4.65	3.48	1.16	4.32	1.81	4.60	2.16
Tm	0.29	0.46	0.30	0.94	0.73	0.98	0.35	0.67	0.52	0.17	0.64	0.26	0.69	0.31
Yb	1.87	3.05	1.98	5.9	4.65	6.3	2.25	4.36	3.43	1.12	4.06	1.79	4.53	1.92
Lu	0.29	0.45	0.29	0.86	0.70	0.95	0.34	0.63	0.52	0.16	0.60	0.27	0.65	0.27
Y	18.4	27.3	20.7	68	49.5	69	23.6	46.3	35.2	11.6	43.7	19.0	45.5	21.6
Th	1.02	0.21	0.61	0.41	0.20	0.43	0.69	0.29	0.16	0.03	1.37	0.85	0.30	0.45
U	0.09	0.22	0.15	0.29	0.29	1.20	0.18	0.11	0.19	0.52	0.12	0.25	0.22	0.15
Zr	6.6	16.3	6.1	5.4	3.19	6.4	4.78	9.1	15.6	10.4	144	87	112	91
Hf	0.40	0.83	0.38	0.34	0.20	0.32	0.19	0.60	0.86	0.47	3.15	1.88	2.93	2.38
Nb	1.28	2.60	3.04	6.0	0.89	5.2	2.48	4.26	1.89	0.78	23.8	10.2	4.68	7.3
Ta	0.06	0.12	0.16	0.37	0.07	0.30	0.15	0.25	0.11	0.03	1.24	0.55	0.23	0.49
Sc	57	45.3	33.5	40.0	42.9	44.4	29.9	45.9	45.8	35.2	53.5	24.7	24.1	28.6
V	463	296	240	509	413	563	283	396	348		356	171	331	278

(Continued)

Table 3. (Continued)

	SFM-1	SFM-6	F-9	F-12	MT.DIAB-1	HW-GABB	YR 44	YR 45	FR 92-4	GT/GL (1)	R/GT	TIBB-R
	Franciscan Low-Grade Rocks				Coast Range Ophiolites		Feather River Ultramafic Belt Amphibolites				Rinds	
Rb	5.1	1.32	0.44	0.24	1.04	0.17	16.0	5.9	11.6	1.43	3.93	54.78
Ba	45	15.5	222	38	11	4	161	53	79	46.05	84.71	1474.89
Sr	504	244	44	89	56	142	139	156	86	12.98	14.40	44.38
Pb	2.01	1.08	0.96	0.92	107	0.19	13.5	3.63	8.62	3.13	2.32	2.57
La	6.6	5.3	5.7	7.11	4.64	0.08	1.18	1.6	2.07	0.77	0.08	0.74
Ce	24.1	17.5	17.4	21.5	13.6	0.2	3.32	4.31	5.41	1.73	0.36	2.37
Pr	4.10	3.02	3.00	3.63	2.35	0.06	0.68	0.82	0.95	0.27	0.10	0.28
Nd	21.6	15.8	15.9	19.1	12.4	0.37	4.25	4.91	5.28	1.27	0.70	1.48
Sm	7.5	5.3	5.5	6.5	4.40	0.18	2.11	2.21	2.19	0.45	0.34	0.97
Eu	2.64	1.76	1.87	2.19	1.67	0.20	0.93	0.92	0.86	0.15	0.13	0.52
Gd	10.2	7.2	7.4	8.6	6.1	0.41	3.00	3.34	2.79	0.60	0.40	1.01
Tb	1.79	1.31	1.30	1.54	1.12	0.08	0.66	0.75	0.53	0.14	0.10	0.21
Dy	11.3	8.4	8.2	9.8	7.3	0.57	4.86	5.61	3.79	0.93	0.65	1.40
Ho	2.40	1.82	1.82	2.11	1.61	0.13	1.13	1.31	0.94	0.20	0.14	0.34
Er	6.3	4.96	5.1	5.8	4.63	0.38	3.15	3.72	2.95	0.58	0.45	1.07
Tm	0.88	0.74	0.75	0.84	0.70	0.06	0.49	0.59	0.53	0.09	0.07	0.17
Yb	5.4	4.49	4.80	5.2	4.55	0.38	3.36	4.09	3.66	0.56	0.50	1.22
Lu	0.66	0.59	0.66	0.70	0.68	0.06	0.49	0.61	0.56	0.08	0.07	0.19
Y	65	48.3	51	58	43.9	3.2	33.0	38.4	30.3	5.11	4.36	9.89
Th	0.46	0.63	0.23	0.26	0.36	0.05	0.12	0.14	0.18	0.20	0.03	0.39
U	0.20	0.47	0.09	0.16	0.18	0.00	0.03	0.03	0.11	0.02	0.01	0.09
Zr	47.7	57	70	55	124	1.5						
Hf	2.11	1.86	2.21	1.84	3.47	0.07	0.61	0.50	0.43			
Nb	6.3	5.6	4.22	3.22	4.61	0.07	1.29	1.65	1.58	0.53	0.03	0.95
Ta	0.36	0.24	0.27	0.17	0.25	0.05	0.09	0.13	0.10	0.78	0.18	0.90
Sc	66.2	40.6	46.2	44.4	48.4	60	72	67	36.4			
V	434	483	419	429	394	1007	348	365	430			

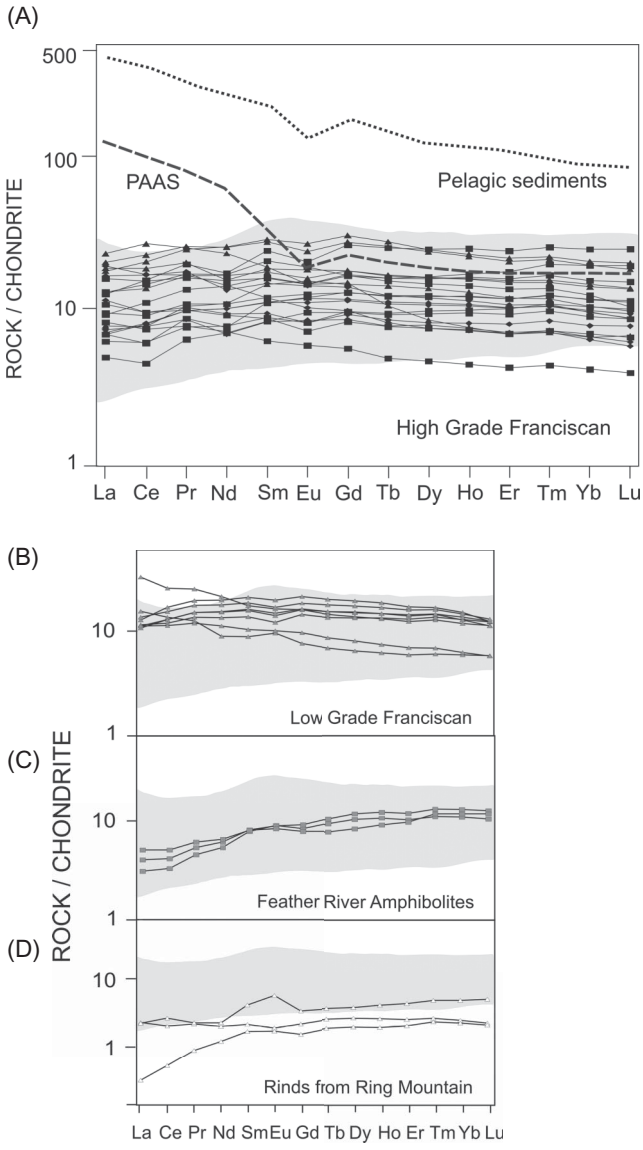

Figure 6. Chondrite-normalized REE patterns of (A) high-grade Franciscan rocks and (B) low-grade Franciscan coherent rocks, (C) high-grade Feather River amphibolites, and (D) rinds from Ring Mountain. The shaded region is a summary of Western Pacific arc tholeiite data (Jakes and Gill 1970). *Post*-Archaean Australian Shale (PAAS) from Taylor and McLennan (1985) and pelagic sediments from Plank and Langmuir (1998). Symbols are as in Figure 2.

their inferred formational ages (Wakabayashi *et al*. 2010). The Pb-isotopic ratios of these rocks are compared with those of three intra-oceanic arcs of the Western Pacific (Figure 11), the Mariana, Kurile, and Izu-Bonin arcs, and the Pacific MORB (GEOROC database, Max Planck Institute). Various mantle reservoirs and the Northern Hemisphere Reference Line (NHRL) are also plotted for reference (Figure 11). Franciscan Pb data are similar to the Izu-Bonin and Mariana arcs (Pearce *et al*. 1992) even though they also fall partially within the field of Pacific MORB (Church and Tatsumoto 1975; Tatsumoto 1978; White *et al*. 1987; Hanan and Schilling 1989). All these rocks show a steeper trend than the NHRL and are similar to those of the Western Pacific arc rocks. Note that low-grade rocks plot closer to the NHRL (compared to all high-grade rocks) with their Pb isotopes similar to both Pacific MORB and Izu-Bonin Arc, but with a greater correlation to Pacific MORB (from REE data, Figure 6).

Nd–Sm systematics data of the rocks of this study are reported in Table 4. Note the initial ε_{Nd} are calculated at 195–130 million years (Table 4), the ages of formation of the respective protoliths that are not necessarily genetically related. In Figure 12, these $\varepsilon_{Nd(I)}$ are plotted against Th/La for all the Franciscan rocks and the FRB amphibolites. It is noteworthy that the low-grade Franciscan rocks and the high-grade Feather River rocks, both of supposedly MORB parentage as discussed later, show a relatively restricted range of composition in this plot (Figure 12), compared with the high-grade Franciscan rocks.

Discussion

Major element variation of the Franciscan metamorphic rocks

It is generally accepted that the major element chemical composition of a rock changes little except for a few elements during subduction metamorphism or during seafloor hydrothermal metamorphism of basalts prior to subduction (VonDamm *et al*. 1985). To assess the mobility of Na, K, and Si in these rocks and to distinguish mobility during subduction-related metamorphism from original protolith composition of the rocks with our geochemical data, the degree to which metamorphism may have affected the geochemical signature needs to be evaluated.

The major element compositions of Franciscan rocks are remarkably consistent despite their diverse spatial and metamorphic relations. Although the total alkali silica plot (Figure 2) does not distinguish calc-alkaline from tholeiitic because tholeiitic basalt is a member of the calk-alkaline suite of rocks, for our high-grade rocks of this study silica and (Na_2O+K_2O) positively correlate along the basalt, trachy-basalt, and basaltic trachy-andesite fields. This trend is similar to the calc-alkaline trend of arc rocks. The above-mentioned calc-alkaline trend is absent for the low-grade rocks of this study.

The conventional total alkali versus SiO_2 wt.% plot indicates enrichment in Na and K and both enrichment and depletion in SiO_2 relative to the basalt field. Metasomatic processes associated with blueschist, eclogite, and amphibolite facies metamorphism (Sorensen *et al*. 1997) and palagonitization within the top few hundred metres of the ocean floor may cause enrichment in K (Ridley *et al*. 1994). Na enrichment in rocks due to spilitization of the ocean floor is also common. However, the data show no

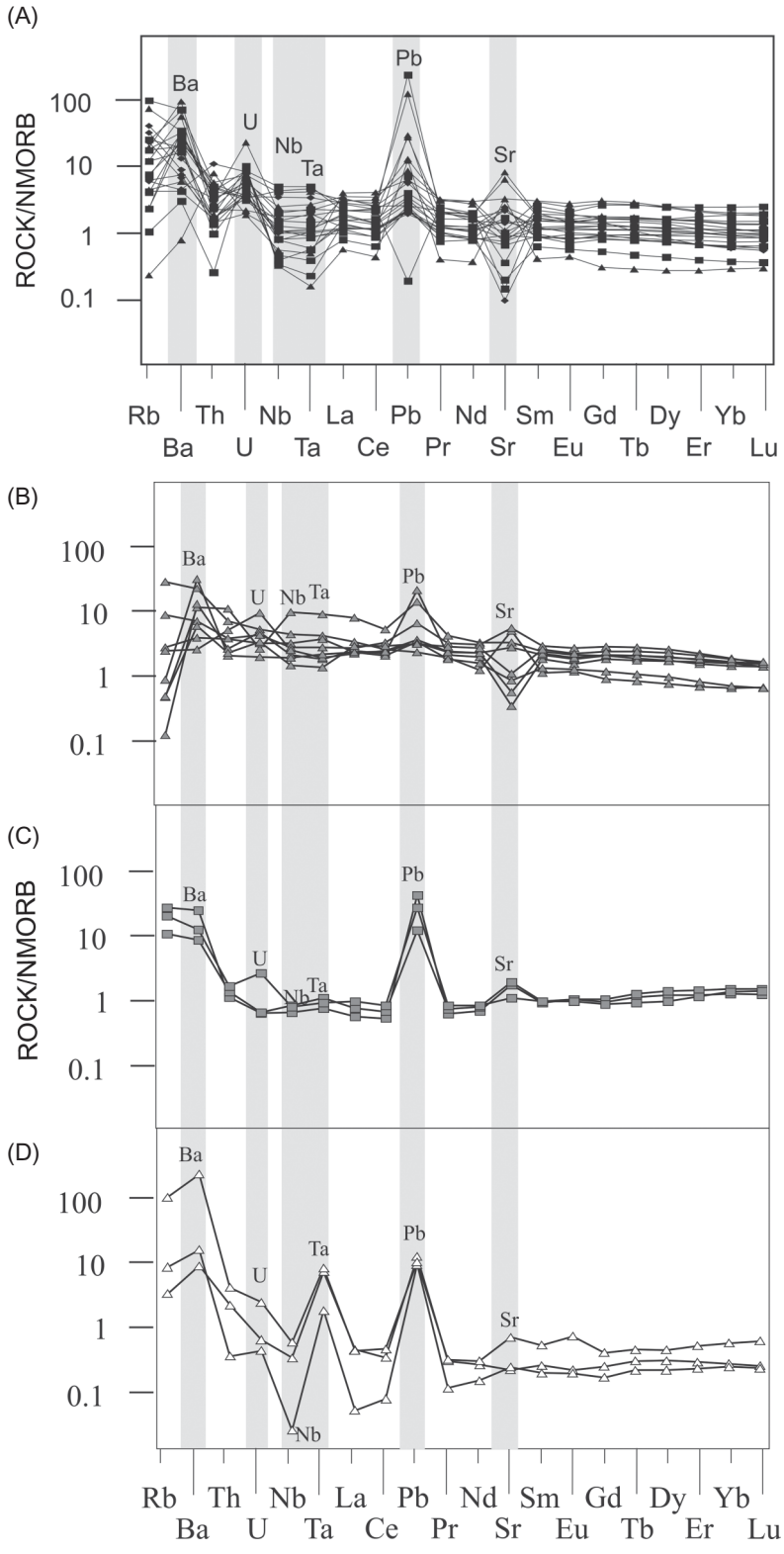

Figure 7. Multiple trace element concentrations normalized over N-MORB for (A) high-grade Franciscan rocks and (B) low-grade Franciscan rocks, (C) high-grade Feather River amphibolites, and (D) rinds from Ring Mountain. Elements are arranged according to varying incompatibility (Sun and McDonough 1989; Tatsumi and Eggins 1995). Symbols are as in Figure 2.

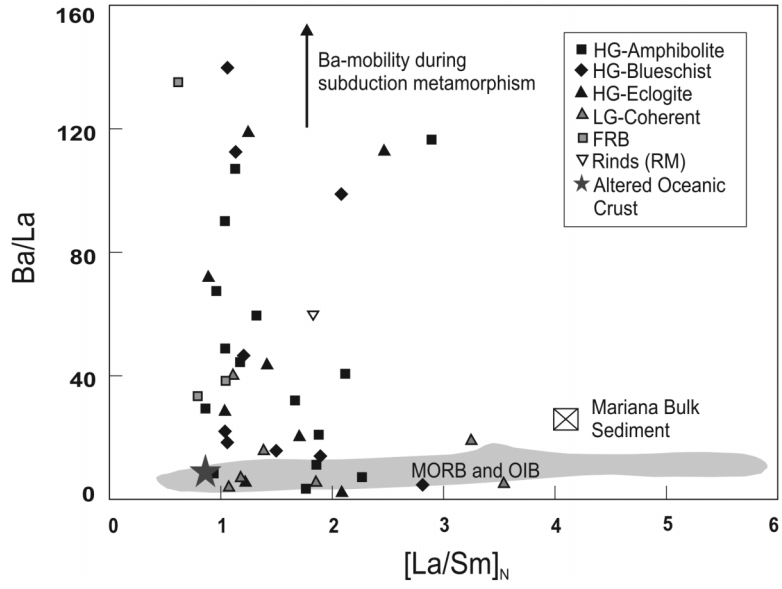

Figure 8. Variation of Ba/La with $[La/Sm]_N$ (normalized to chondrite) in the Franciscan [including data from Saha *et al.* (2005) and Wakabayashi *et al.* (2010)] and Feather River rocks. Mariana bulk sediment – from hole 801 of ODP leg 129 (Elliott *et al.* 1997). Field of MORB and OIB are from Kent and Elliott (2002). Altered oceanic crust data from Nakamura *et al.* (2007). Only one rind data plots in this figure with other rinds have Ba/La ratios >160 (Table 2). FRB, Feather River ultramafic belt; HG, Franciscan high-grade rocks; LG, Franciscan low-grade coherent rocks; RM, Ring Mountain locality.

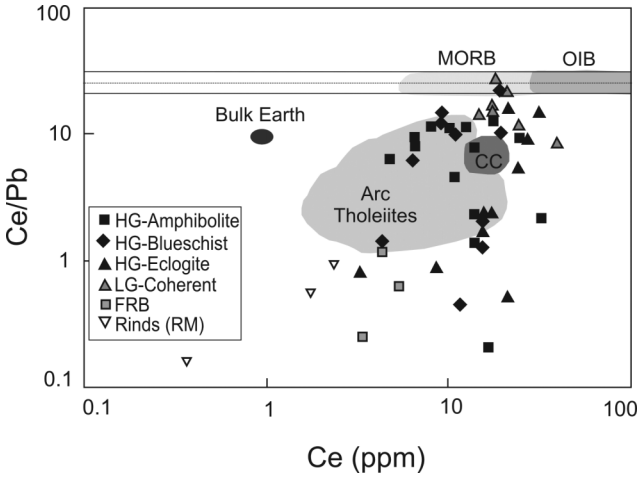

Figure 9. Ce/Pb ratios and Ce concentrations in the Franciscan rock samples of this study, compared with fields for oceanic basalts (MORB and OIB), global arc lavas, continental crust (CC), and bulk earth (data fields as in Saha *et al*. 2005, and references therein). FRB, Feather River ultramafic belt; HG, Franciscan high-grade rocks; LG, Franciscan low-grade coherent rocks; RM, Ring Mountain locality.

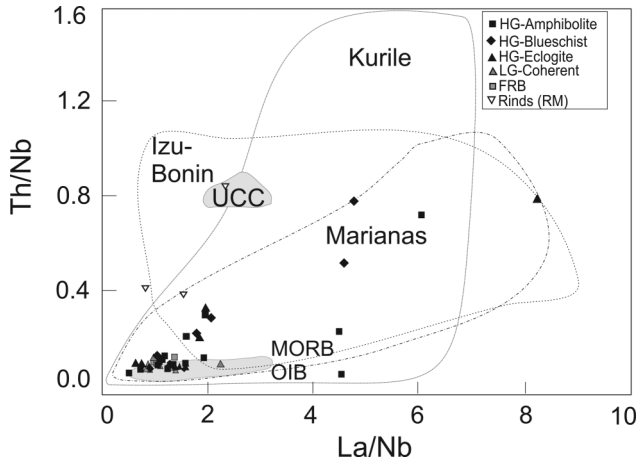

Figure 10. Ratios of Th/Nb versus La/Nb for the high- and low-grade Franciscan, CRO (Coast Range ophiolite), and FRB (Feather River ultramafic belt) rocks of this study. Fields of MORB–OIB and upper continental crust (UCC) are from Plank (2005) and references therein. Fields of Mariana, Izu-Bonin, and Kurile intra-oceanic arcs are from GEOROC (http://georoc.mpch-mainz.gwdg.de/Entry.html). FRB, Feather River ultramafic belt; HG, Franciscan high-grade rocks; LG, Franciscan low-grade coherent rocks; RM, Ring Mountain locality.

systematic variation with increasing metamorphic grade (Figure 2) and no correspondence between K_2O enrichment and metamorphic grade (Figure 3), so it is more likely that the variability in Na_2O and K_2O of our samples reflects protolith variability rather than mobilization during subduction metamorphism.

Nearly half the samples of this study have SiO_2 wt.% less than average seafloor basalts (~48%) (Lofgren *et al*. 1979). This depletion of silica in these metamorphic rocks can be due to hydrothermal alteration and metamorphism of the protolith rock on the seafloor before subduction

Table 4. Sm, Nd, U, Th, Pb systematics data, and initial Nd–Pb isotopic ratios at 195–130 Ma for rocks of the Franciscan Complex and 240 Ma for the Feather River ultramafic complex rocks.

	GM-1	GM-2	GM-3	F-3	WC-SSS-1	WC-MV-1	WC-MV-2	95-DIAB-14	95-DIAB-29	95-DIAB-031	95-DIAB-107C	CSUH-1	SUNOL-2038	JS-Ecg
	High-grade Franciscan Rocks (169 Ma)													
Sm (ppm)	2.25	3.30	7.01	4.50	4.13	3.07	3.04	3.27	2.23	5.20	4.07	5.93	1.06	5.39
Nd (ppm)	5.70	9.1	15.0	13.4	11.4	8.50	8.50	12.4	5.60	13.5	9.20	14.7	2.65	20.63
$^{147}Sm/^{144}Nd$	0.22	0.23	0.24	0.21	0.19	0.23	0.22	0.17	0.20	0.19	0.25	0.23	0.20	0.17
$^{143}Nd/^{144}Nd_{(0)}$	0.513132	0.513041	0.513082	0.512947	0.512951	0.513044	0.512954	0.512949	0.513029	0.512920	0.512895	0.513179	0.512949	0.512697
$^{143}Nd/^{144}Nd_{(I)}$	0.512886	0.512792	0.512818	0.512711	0.512746	0.512793	0.512707	0.512765	0.512806	0.512707	0.512623	0.512920	0.512731	0.512514
$\varepsilon_{Nd(I)}$	9.1	7.2	7.8	5.7	6.3	7.3	5.6	6.7	7.5	5.6	4.0	9.8	6.1	1.8
U (ppm)	0.21	0.25	0.43	0.16	0.17	0.18	0.10	0.42	0.16	0.38	0.39	0.32	0.47	0.09
Th (ppm)	0.12	0.43	0.54	0.64	0.53	0.20	0.18	1.42	0.21	0.73	0.37	0.30	0.23	1.02
Pb (ppm)	0.73	0.87	0.06	1.27	0.81	0.60	0.70	1.80	0.69	43.0	9.85	12.5	4.05	2.03
$^{206}Pb/^{204}Pb_{(0)}$	21.02	19.09	–	19.03	–	18.75	18.44	18.95	18.68	18.65	18.46	–	–	18.47
$^{207}Pb/^{204}Pb_{(0)}$	15.72	15.64	–	15.64	–	15.55	15.55	15.61	15.57	15.59	15.60	–	–	15.56
$^{208}Pb/^{204}Pb_{(0)}$	39.27	38.56	–	38.82	–	37.96	37.36	38.73	38.07	38.39	38.23	–	–	38.35
$^{238}U/^{204}Pb$	25.67	19.99	–	8.26	–	24.89	8.30	15.35	11.57	0.56	2.51	–	–	2.82
$^{235}U/^{204}Pb$	0.19	0.15	–	0.06	–	0.18	0.06	0.11	0.08	0.00	0.02	–	–	0.02
$^{232}Th/^{204}Pb$	21.21	31.33	–	33.28	–	19.63	13.18	54.38	14.94	1.08	1.95	–	–	32.91
$^{206}Pb/^{204}Pb_{(I)}$	19.34	18.56	–	18.81	–	18.09	18.22	18.54	18.38	18.64	18.39	–	–	18.39
$^{207}Pb/^{204}Pb_{(I)}$	15.72	15.61	–	15.62	–	15.51	15.54	15.59	15.55	15.59	15.59	–	–	15.56
$^{208}Pb/^{204}Pb_{(I)}$	38.78	38.05	–	38.28	–	37.65	37.15	37.85	37.83	38.38	38.20	–	–	37.82

	HPSZ-META	F-1	F-4	F-6	F-8	F-10	F-11	MP-1	TL-4	NR-GABB	NR-PB	MHPB
	High-grade Franciscan rocks (169 Ma)									Franciscan low-grade rocks		
										145 Ma	145 Ma	195 Ma
Sm (ppm)	2.39	2.34	8.06	4.56	8.40	2.55	4.97	3.03	1.64	6.03	2.69	4.54
Nd (ppm)	6.40	7.62	22.77	12.13	22.93	7.82	14.43	6.30	5.87	23.7	8.40	13.73
$^{147}Sm/^{144}Nd$	0.27	0.19	0.22	0.24	0.23	0.21	0.22	0.25	0.18	0.16	0.16	0.21
$^{143}Nd/^{144}Nd_{(0)}$	0.513051	0.512786	0.513123	0.513185	0.513132	0.512885	0.512885	0.513072	0.512983	0.512907	0.512910	0.513101
$^{143}Nd/^{144}Nd_{(I)}$	0.512756	0.512571	0.512875	0.512922	0.512876	0.512657	0.512644	0.512792	0.512781	0.512751	0.512758	0.512837
$\varepsilon_{Nd(I)}$	6.6	2.9	8.9	9.8	8.9	4.6	4.4	7.2	7.0	5.8	5.9	8.7

(Continued)

Table 4. (Continued).

	HPSZ-META	F-1	F-4	F-6	F-8	F-10	F-11	MP-1	TL-4	NR-GABB	NR-PB	MHPB	
U (ppm)	0.22	0.15	0.29	0.29	1.20	0.18	0.11	0.19	0.52	0.12	0.25	0.22	
Th (ppm)	0.21	0.61	0.41	0.20	0.43	0.69	0.29	0.16	0.03	1.37	0.85	0.30	
Pb (ppm)	0.79	2.26	2.78	1.09	4.23	1.02	9.19	0.66	0.66	4.48	0.67	6.89	
$^{206}Pb/^{204}Pb_{(0)}$	18.67	18.65	18.67	18.90	18.89	18.80	18.43	18.79	18.39	18.89	19.66	19.97	
$^{207}Pb/^{204}Pb_{(0)}$	15.65	15.64	15.61	15.57	15.56	15.63	15.57	15.64	15.61	15.65	15.62	15.77	
$^{208}Pb/^{204}Pb_{(0)}$	38.36	38.55	38.35	38.14	38.12	38.52	38.19	38.30	38.21	38.48	38.64	39.14	
$^{238}U/^{204}Pb$	18.85	4.29	6.64	16.89	18.00	11.28	0.74	15.09	13.52	20.18	9.28	1.94	
$^{235}U/^{204}Pb$	0.14	0.03	0.05	0.12	0.13	0.08	0.01	0.11	0.10	0.15	0.07	0.01	
$^{232}Th/^{204}Pb$	17.19	17.84	9.72	11.93	6.69	44.61	2.03	12.72	45.62	65.66	14.53	2.45	
$^{206}Pb/^{204}Pb_{(I)}$	18.17	18.54	18.49	18.45	18.41	18.51	18.41	18.39	18.03	18.43	19.45	19.91	
$^{207}Pb/^{204}Pb_{(I)}$	15.62	15.63	15.60	15.55	15.54	15.62	15.57	15.62	15.59	15.63	15.61	15.76	
$^{208}Pb/^{204}Pb_{(I)}$	38.08	38.26	38.19	37.95	38.02	37.80	38.15	38.10	37.47	37.57	38.44	39.09	

	PAC-1	SFM-1	SFM-6	F-9	F-12	MT.DIAB-1	HW-GABB	YR 44	YR 45	FR 92-4	GT/GL (1)	R/GT	TIBB-R
	Franciscan Low-Grade Rocks					Coast Range Ophiolites (169 Ma)		Feather River Ultramafic Belt Amphibolites (240 Ma)			Rinds (169 Ma)		
	130 Ma	140 Ma	140 Ma	140 Ma	140 Ma								
Sm (ppm)	3.25	7.48	5.31	5.53	6.47	4.40	0.18	2.11	2.21	2.19	0.45	0.34	0.97
Nd (ppm)	10.9	21.6	15.81	15.9	19.1	12.40	0.37	4.25	4.91	5.28	1.27	0.70	1.48
$^{147}Sm/^{144}Nd$	0.19	0.22	0.22	0.22	0.21	0.22	0.37	0.31	0.28	0.26	0.223	0.304	0.41
$^{143}Nd/^{144}Nd_{(0)}$	0.512978	0.513053	0.513208	0.513247	0.513279	0.513049	–	–	0.513164	0.513184	0.512773	0.512992	0.512915
$^{143}Nd/^{144}Nd_{(I)}$	0.512817	0.512855	0.513010	0.513046	0.513083	0.512801	–	–	0.512717	0.512834	0.512525	0.512652	0.512457
$\varepsilon_{Nd(I)}$	6.8	7.7	10.8	11.5	12.2	7.4	–	–	7.6	9.9	2.0	4.7	1.2
U (ppm)	0.45	0.20	0.47	0.09	0.16	0.18	< 0.01	0.03	0.03	0.11	0.02	0.01	0.09
Th (ppm)	0.15	0.46	0.63	0.23	0.26	0.36	0.05	0.12	0.14	0.18	0.20	0.03	0.39
Pb (ppm)	0.99	2.01	1.08	0.96	0.92	106.80	0.19	13.5	3.63	8.62	3.13	2.32	2.57
$^{206}Pb/^{204}Pb_{(0)}$	18.20	18.60	18.58	18.70	18.78	20.15	–	–	–	–	18.38	18.25	18.49
$^{207}Pb/^{204}Pb_{(0)}$	15.48	15.50	15.52	15.56	15.51	15.88	–	–	–	–	15.51	15.52	15.47
$^{208}Pb/^{204}Pb_{(0)}$	37.85	38.03	37.99	38.22	38.00	39.55	–	–	–	–	37.87	37.84	38.02
$^{238}U/^{204}Pb$	10.20	6.71	6.03	5.89	10.65	0.11	–	–	–	–	0.42	0.38	2.16
$^{235}U/^{204}Pb$	0.07	0.05	0.04	0.04	0.08	0.00	–	–	–	–	0.01	0.01	0.02
$^{232}Th/^{204}Pb$	29.86	14.22	9.72	15.99	18.74	0.23	–	–	–	–	4.16	0.81	9.86
$^{206}Pb/^{204}Pb_{(I)}$	17.99	18.45	18.44	18.57	18.55	20.15	–	–	–	–	18.37	18.24	18.43
$^{207}Pb/^{204}Pb_{(I)}$	15.47	15.49	15.51	15.55	15.50	15.88	–	–	–	–	15.50	15.52	15.47
$^{208}Pb/^{204}Pb_{(I)}$	37.39	37.84	37.86	38.01	37.75	39.55	–	–	–	–	37.81	37.83	37.87

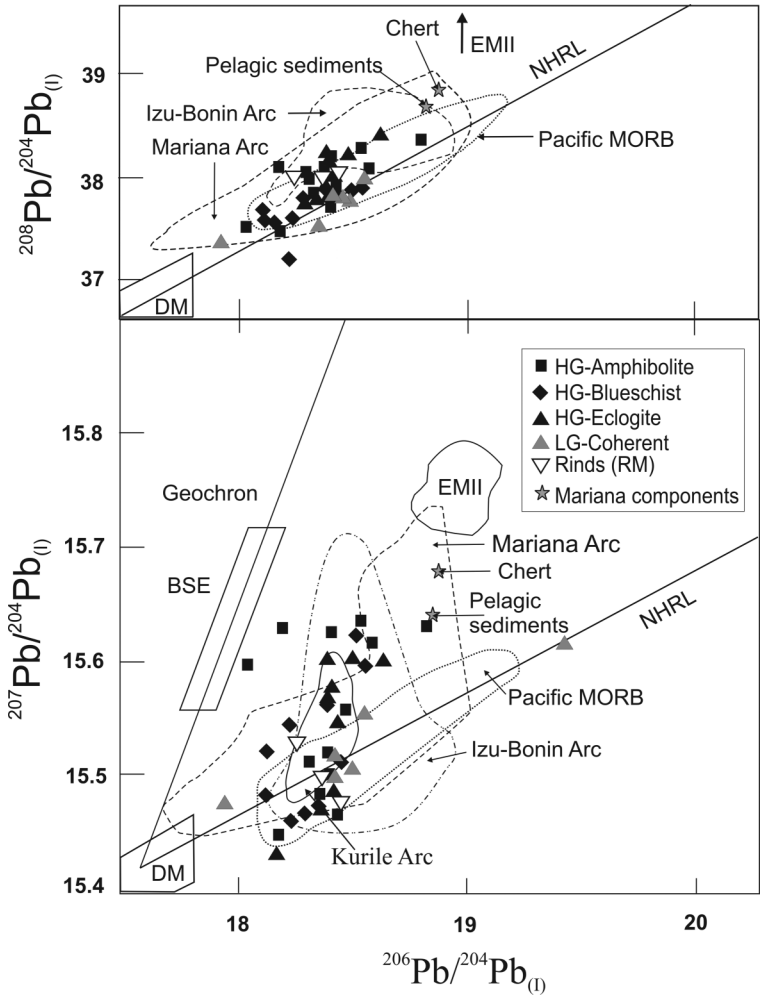

Figure 11. Initial Pb-isotopic compositions of the Franciscan rocks (Table 4), compared with Pb-isotopic ratios of three intra-oceanic arcs of the Western Pacific. These arc data are from various sources and compiled by the Max Planck Data Sources (http://georoc.mpch-mainz.gwdg.de/Entry.html). Mariana chert and Mariana pelagic sediments are from Plank and Langmuir (1998). HG, Franciscan high-grade rocks; LG, Franciscan low-grade coherent rocks; RM, Ring Mountain locality.

(Bowers *et al*. 1985) or it can also be caused by metamorphic reactions such as albite → jadeite + quartz during subduction. If silica is lost during subduction metamorphism, then the higher grade rocks are expected to have experienced greater silica loss. Figure 3A shows the variation of SiO_2 wt.% with metamorphic grade. There is no systematic correlation of silica with increasing metamorphic grade (Figures 2, 3A, and 4), indicating that Si depletion is not due to subduction metamorphism. This depletion must have been inherited in the protolith by the hydrothermal alteration on the seafloor. The concentration of silica in the circulating hydrothermal fluid on the seafloor is probably controlled by the solubility of quartz. SiO_2 is generally removed into solution during this process and most hydrothermally altered rocks show a loss of silica (VonDamm *et al*. 1985). This has been shown to be the case in Reykjavik geothermal systems (Arnorsson 1970). Our conclusion that silica depletion resulted from seafloor metamorphism is consistent with the study of Philippot *et al.* (1998), who concluded that differences in salt contents in fluid inclusions from different HP terranes (including the Franciscan) were inherited from seafloor hydrothermal metamorphism.

There is a small degree correlation of K_2O wt.% with increasing metamorphic grade (Figure 3B) for rocks with $<1.5\%$ K_2O; however, high potassium content ($>1.5\%$) in some of the rocks can be better explained by high potassium content in their parent rocks. Although K_2O in the high-grade rocks may have been mobilized due to subduction metamorphism, the possibility that the high-grade rocks had high K_2O values prior to subduction cannot be ruled out.

It is clear from Figure 4 that the low-grade rocks do not show much chemical variation and their observed major element composition is essentially within the wider chemical range of the high-grade rocks, except for Na_2O. If

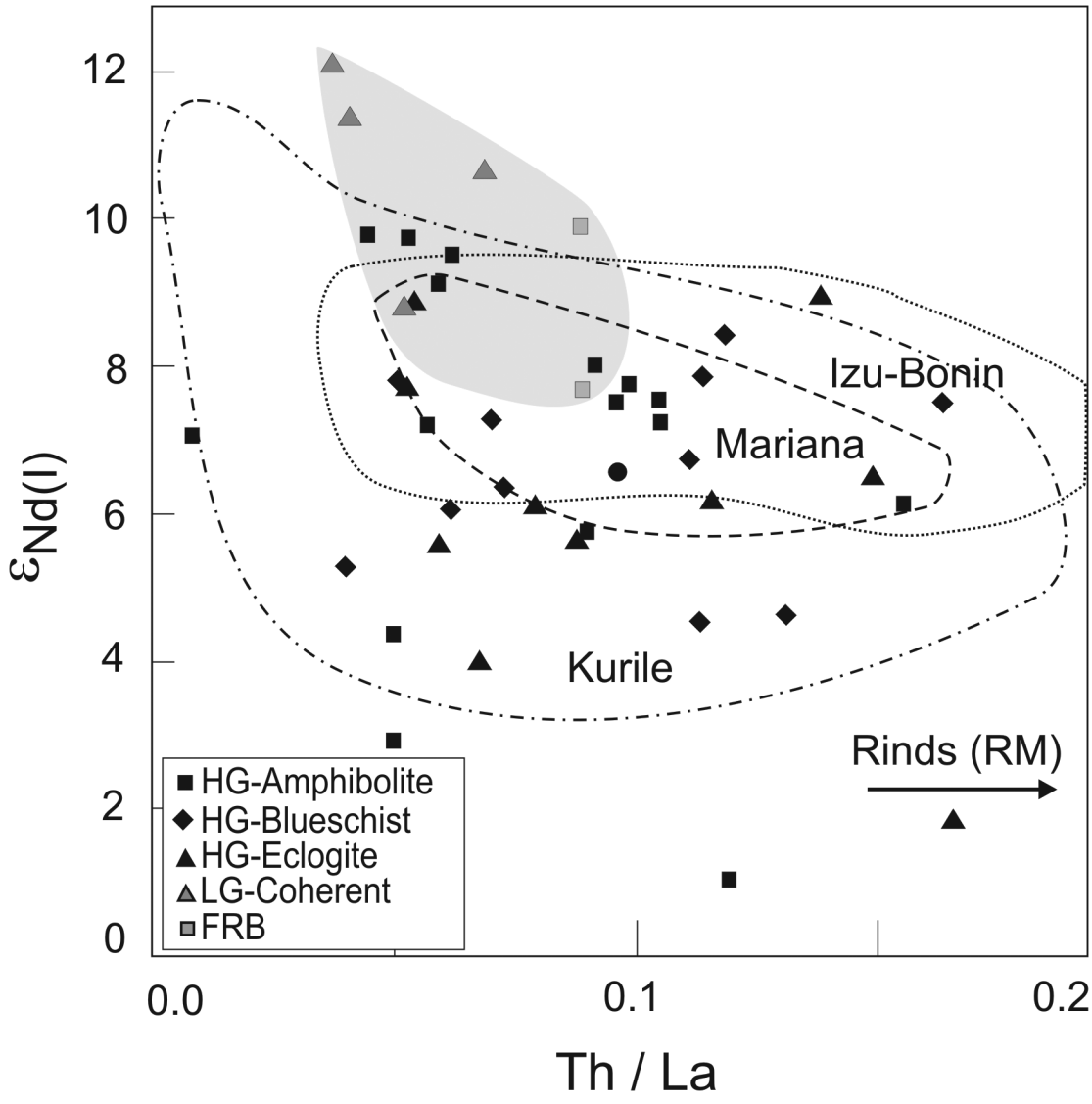

Figure 12. Initial ε_{Nd} (Table 4) versus Th/La of the Franciscan and Feather River rocks compared with Izu-Bonin, Kurile, and Mariana arcs. The shaded region represents rocks of MORB protolith from Franciscan and Feather River complexes. Rinds from Ring Mountain fall outside the scale of this figure with $\varepsilon_{Nd(I)}$ ranging from 1.2 to 4.7 (Table 4) and Th/La ranging from 0.26 to 0.56. FRB, Feather River ultramafic belt; HG, Franciscan high-grade rocks; LG, Franciscan low-grade coherent rocks; RM, Ring Mountain locality.;

subduction metamorphism was the cause of larger variation in the high-grade rocks, the chemical shift would be expected to be systematic in one direction due to prograde metamorphism. However, the observed radial pattern in chemical variation of the high-grade rocks (Figure 4) does not show any unique trend. Nor is there any evidence of a systematic change in chemical variation with increasing metamorphic grade. It appears that the low-grade rocks have retained their protolith bulk compositions of igneous parentage. The high-grade rocks, on the other hand, showing larger variation in major element compositions, may indicate magmatic crystal fractionation in the protolith rocks that are consistent with fractional crystallization of pyroxenes and Fe–Ti oxides, without any olivine or plagioclase removal. This crystal fractionation scenario is discussed below with respect to the relevant major oxide variations (Figure 4).

Decrease in FeO* wt.% with increasing silica (Figure 4) is indicative of magmatic fractionation of a mafic mineral phase that could be either olivine or pyroxene. The lack of any discernible variation in MgO wt.% with changing SiO_2 wt.% may imply minimal olivine or orthopyroxene fractionation. Reduction of CaO with increasing SiO_2 content may be due to the removal from the melt of either clinopyroxenes or plagioclase or both. The variation of CaO/Al_2O_3 with increasing SiO_2 suggests magmatic

fractionation of clinopyroxene. From our REE data (discussed later), we can confirm the absence of any plagioclase fractionation due to the lack of a Eu-anomaly.

The bulk rocks show no significant variation in P_2O_5 contents (Figure 4) that are low except for two samples. The high P_2O_5 contents in two high-grade rocks may be due to seafloor alteration of glassy material (Murton *et al*. 1992), because these two rocks do not have any chert component (Appendix). Decrease in TiO_2 with increasing silica may be due to the fractionation of Fe–Ti oxide phases.

The high-grade rocks of this study are similar to a calc-alkaline evolutionary trend with lower FeO* values for a given Mg # (Figure 5). Although Ti and Fe show comparable variation in low-grade and high-grade rocks, Ti shows a much steeper and distinctly negative slope against increasing Mg # for the high-grade rocks. This is clearly indicative of Fe–Ti oxide fractionation in the protolith magma. The increase in TiO_2 wt.% for evolved high-grade (Figure 5) rocks suggests igneous TiO_2 fractionation rather than a subduction-induced metamorphic process. The protoliths of these high-grade rocks apparently had Ti-rich minerals that were metamorphosed to form new minerals during closed-system subduction metamorphism.

It is clear from the above discussion that the variability in major element compositions of Franciscan rocks reflects protolith variations resulting from igneous processes rather than element mobility during metamorphism. A more rigorous evaluation of element mobility versus protolith geochemical signatures is given below in the assessment of REE data that suggests no exchange with continent-derived sediments. Other trace element data indicate different protolith signatures for high- and low-grade Franciscan and high-grade Feather River rocks.

Rare earth and other trace elements

In general, mobility of elements is expected to increase with increasing grade of metamorphism (e.g. Bebout *et al*. 1993; Bebout 1995). For our samples, it is expected that low-grade rocks should show less elemental mobility relative to high-grade rocks. FRB amphibolites with MORB protoliths (as discussed below) and the arc protoliths of Franciscan high-grade rocks (Saha *et al*. 2005; Wakabayashi *et al*. 2010) should show similar degrees of elemental mobility. Differential elemental retention for similar high-grades of metamorphism of MORB and arc protoliths is useful in distinguishing original protolith trace element composition versus modified trace element composition due to varying degrees of mobility of various elements during subduction metamorphism.

The REE patterns of most of the high-grade Franciscan rocks (Figure 6A) fall in the field of Western Pacific arc tholeiites and their overall patterns are essentially flat and similar to nascent intra-oceanic arc basalts (Hawkesworth *et al*. 1977; Tatsumi and Eggins 1995). These rocks are distinctly different from OIB and enriched MORB (E-MORB) that are LREE enriched relative to the HREEs. As the characteristic LREE enrichment of PAAS and pelagic sediments are clearly absent in the REE patterns of the Franciscan rocks (Figure 6A), we can rule out continental crustal/pelagic sediment contamination in these rocks. This is an important conclusion that is further strengthened by comparison of other geochemical data, as discussed below, of the high-grade Franciscan rocks with the PAAS and Pacific Ocean pelagic sediments. It is noteworthy that the FRB amphibolites are strikingly different from the Franciscan high- and low-grade rocks (Figure 6B). The FRB rocks show a notable depletion of the LREEs similar to normal mid-ocean ridge basalts. Clearly, there was no LREE mobility in these rocks during subduction metamorphism.

In Franciscan rocks, there is a distinct difference in the REE patterns between the MORB-like low-grade rocks with LREE depletion (except the two OIB-like samples from Nicasio and Pacifica) and the high-grade rocks that are relatively flat. The depleted LREE patterns for low-grade rocks would have been erased had there been any elemental mobility during subduction. However, the characteristic LREE depletion seen in the low-grade MORB rocks (Figure 6B) implies that there was little elemental mobility in these rocks during subduction.

High-grade Franciscan rocks could have either an arc protolith or a MORB protolith with a very small degree of LREE enrichment making their patterns flat (Figure 6A). If the latter were the case, then FRB amphibolites should also show flat or less depleted LREEs as both these rock groups have undergone similar high-grade metamorphism. More importantly, the mobility of LREEs does not obliterate the primary composition of rocks that have undergone high grades of metamorphism up to the amphibolite facies.

Multiple trace element patterns normalized to N-MORB are shown in Figure 7. N-MORB-normalized trace element patterns characteristic of arcs have Nb depletion, high concentrations of Ba and Pb, and high Ba/Rb, Ba/Th, U/Th, U/Nb, and La/Nb ratios. Franciscan high-grade rocks show these characteristic arc signatures with high Ba and Pb concentrations. The typical arc-like trace element signatures for Franciscan high-grade rocks are absent in the low-grade rocks (Figure 7B), implying a different non-arc protolith for the latter. FRB amphibolites show a generally flat pattern when normalized to N-MORB except for higher Ba, U, and Pb concentrations (Figure 7B). Therefore, the observed enrichment of Ba, U, and Pb in FRB rocks must be due to later mobilization of these elements during subduction metamorphism of a MORB protolith.

FRB amphibolites underwent metamorphism comparable to Franciscan high-grade rocks. Despite their high grade of metamorphism, the FRB amphibolites still maintain a relatively flat pattern when normalized to N-MORB

for a majority of the elements in Figure 7B. Given the similar high-grade metamorphism in these two rock groups, we infer that there was no trace element mobilization during metamorphism except for Ba, Pb, and U. The negative Nb–Ta anomaly seen only in the high-grade Franciscan rocks (Figure 7A) must indicate their inheritance from an arc protolith.

Note that the typical arc signatures in the multi-element diagram, including Nb–Ta, are well developed in high-grade Franciscan rocks (Figure 7A). Thus we consider it unlikely that a subducting MORB crust, only by remobilization of the slab fluids, would mimic exactly the trace element signature of an arc as seen in the high-grade Franciscan rocks. The typical arc signatures seen in the high-grade Franciscan rocks reflect protolith composition rather than elemental mobility during subduction metamorphism.

Mobile and immobile trace elements and ratios

Previous studies of trace element behaviour during progressive metamorphism and devolatilization in subducted rocks have indicated the significance of this process in mobilizing selective trace elements (Hart and Staudigel 1989; Weaver 1991; Moran *et al*. 1992; Bebout and Barton 1993; Bebout *et al*. 1993; Ryan and Langmuir 1993; Leeman *et al*. 1994; Bebout 1995). Metabasaltic rocks of the Franciscan and the FRB show some enrichment in elements such as Ba and Pb relative to N-MORB. However, these enrichments in some mobile elements have not destroyed the protolith signatures of these rocks with respect to other less mobile and immobile elements.

The relationship between fluid addition, protolith composition, and the presence or absence of a sedimentary component can be evaluated in a plot of Ba/La against $[La/Sm]_N$ (Figure 8). High-grade Franciscan and FRB samples show high Ba/La and low $[La/Sm]_N$ ratios, indicating the presence of a mobile Ba-rich fluid in the subducting slab. FRB amphibolites of MORB derivation fall outside the fields of MORB and OIB, clearly due to addition of Ba (Figure 8). Most of the low-grade Franciscan rocks fall within the MORB and OIB fields (Figure 8), implying greater mobility of Ba with higher metamorphic grades. It is also notable from Figure 8 that there is no Mariana-type sediment contamination in Franciscan and FRB rocks. Therefore, the observed Ba mobility must be within a closed system of fluid-bearing metabasaltic protoliths.

Ce/Pb ratios are generally remarkably uniform in both MORB and OIBs (Hofmann *et al*. 1986) with a value of 25 ± 5 (Figure 9). Continental crust, however, has a much lower value of 4. The correspondence of most of the high-grade Franciscan data with the arc lavas is clear. However, high-grade FRB amphibolites of MORB protolith (Figures 6C and 7B) show low Ce/Pb ratios falling well below the MORB–OIB field. Both high-grade rock groups show elevated Pb concentrations (Figure 7), causing their Ce/Pb ratio to be lower, as Pb is a fluid-mobile element. Comparison of low-grade Franciscan (Figure 7B) and high-grade FRB rocks (Figure 7B), both of MORB protoliths, suggests increasing mobility of Pb during higher grade metamorphism of the FRB, with much lower Ce/Pb ratios for the latter. It is important to note that although Pb concentrations do not retain the original protolith information of the rocks, the isotopic ratios are not modified by elemental mobility as discussed later. A significant observation from Figure 9 is that low-grade Franciscan rocks show a small range in their Ce/Pb ratios falling close to their expected MORB protolith field. In addition, some of high-grade Franciscan rocks lie close to MORB field. We interpret the higher Ce/Pb ratio of these high-grade rocks by the removal of Pb from a much lower Ce/Pb ratio of their arc protolith.

The ratios of Th/Nb and La/Nb are useful tracers for MORB and OIB, arc lavas, and continental crust (Plank 2005). These tracers can be used as indicators for the presence of these components in a subducting slab. Note that La is the only mobile element in this plot (Figure 10). All the rocks that fall outside the field of MORB and OIB are the high-grade Franciscan rocks with arc parentage (Figure 10). The high-grade FRB samples falling in the field of MORB in this figure do not exhibit any La mobility, considering that Nb is immobile. Rocks falling outside the MORB and OIB fields are enclosed by the fields of various intra-oceanic arcs (Figure 10). These rocks preserve their arc protolith, irrespective of the possible mobility of La during subduction. Another important conclusion is the absence of UCC in any of these rocks, except for one rind that is in the restricted UCC field (Figure 10).

The lack of any component of continentally derived sediment, intra-oceanic arc derived pelagic clay, and volcanoclastic turbidites in the Franciscan and Feather River metavolcanic rocks, irrespective of their grade of metamorphism, is consistent in all our trace element data (Figures 6–106–10). This result indicates a lack of chemical exchange between subducted volcanic rocks and sediments subducted in the same system. The Feather River rocks are structurally interleaved with subordinate, but widespread high-grade metacherts and metaclastic rocks. The Franciscan high-grade rocks have volumetrically small, but ubiquitous, metachert layers or horizons, but no interleaved or coeval (in terms of accretion age) metaclastic rocks. Subduction accretion of Franciscan metaclastic rocks may have begun as early as 144 Ma, but did not take place in significant volumes until about 120 Ma (Dumitru *et al*. 2010). Even our Franciscan samples that were accreted at ca. 120 Ma or later, in an accretionary wedge with large volumes of metaclastic sediments (eight samples), show no evidence of chemical exchange with subducted sediments.

Loss and gain of some trace elements through fluids during subduction metamorphism is suggested for Ba, La, and Pb mobility in our geochemical data as discussed above. However, based on other trace element concentrations and ratios for Franciscan and FRB samples, most of the fluid-induced mobility appears to have occurred in a closed system largely preserving the original bulk-rock composition of the protoliths.

Nd and Pb isotope relations

Devolatilization and preferential mobilization of some fluid-mobile elements result in stable isotope fractionation of oxygen during metamorphism in the subducting slab (e.g. Taylor and Coleman 1968; Bottinga 1969; Chacko *et al*. 1991). Here we evaluate the concentrations and isotopic ratios of lithophile elements Pb and Nd as a function of subduction-zone metamorphism. Their radiogenic isotopic signatures in high- and low-grade Franciscan and FRB rocks show that these elements are still representative of the original protolith despite high mobility of Pb and possible mobility of Nd during subduction.

Arc basalts that display steep arrays in $^{207}Pb/^{204}Pb$ against $^{206}Pb/^{204}Pb$ (Figure 11) are usually interpreted to indicate continental sediment involvement in their genesis (Meijer 1976; Hawkesworth *et al*. 1977; Dickens 1995). We have already inferred that there is no subducted continental sediment contribution in the high-grade Franciscan rocks. If any continental sediment had been present in these rocks, they would have had higher $^{207}Pb/^{204}Pb$ ratios, falling closer or within the field of EM II, as well as having LREE enrichment that we do not observe in these samples. The low-grade rocks of this study notably plot closer to the NHRL with their Pb-isotopic ratios similar to both Pacific MORB and Izu-Bonin Arc volcanics (Figure 11), but with a greater correlation to Pacific MORB (from REE data, Figure 6A).

As we have already discussed, high-grade Franciscan rocks with arc protoliths show Pb-isotopic ratios similar to the intra-oceanic arcs and low-grade Franciscan rocks of MORB derivation plot closer to the NHRL. Although the Pb concentrations of all these Franciscan rocks are modified by fluid mobility, the Pb-isotopic signatures are preserved with remarkable fidelity for the protoliths of these rocks. In other words, Pb was clearly mobile within the closed system of the protolith rocks, without exchanging Pb from any extraneous source during the Franciscan subduction process. Although increasing mobility of Pb with increasing metamorphic grade is indicated in our geochemical data, Pb is redistributed by metamorphic fluids within the closed system of the subducting metabasaltic slab that is indicated by its relatively homogeneous isotopic composition, in contrast with lighter stable isotopes of H and O (Taylor and Coleman 1968; Magaritz and Taylor 1976).

Franciscan and FRB rocks of this study are compared with the Pacific intra-oceanic arcs in a plot of $\varepsilon_{Nd(I)}$ versus Th/La (Figure 12). Most of the high-grade rocks fall within the field of intra-oceanic arcs, such as Izu-Bonin, Mariana, and Kurile arcs. The three samples with lower ε_{Nd} falling outside the field of intra-oceanic arcs have been explained in our previous study as having non-basaltic lithologic components such as radiolarian chert (Wakabayashi *et al*. 2010). Thus, all the rocks in Figure 12 can be interpreted to have had either arc or MORB as their protoliths, with a few samples having a chert component. It should be noted that a similar range of Nd-isotopic data for Franciscan high-grade rocks was also reported by Nelson and DePaolo (Nelson and DePaolo 1985). However, these authors interpreted the low ε_{Nd} samples by a fluid source-derived component of subducted continental sediments (Nelson 1991, 1995). We have already eliminated the possibility of continental crustal components on the basis of the REE data and other trace element concentration and ratio plots (Figures 6, 8, and 10) as well as Pb isotopes (Figure 11) for all the rocks of this study.

The four low-grade rocks from the Franciscan Complex and two FRB amphibolites (Figure 12) have characteristically high MORB-like initial ε_{Nd} values. We have established from our foregoing discussion of trace element data (Figure 6) as well as from previous studies (Saha *et al*. 2005; Wakabayashi *et al*. 2010) that low-grade Franciscan rocks and the FRB amphibolites have a MORB protolith. Thus there is a marked distinction in the initial ε_{Nd} values between the MORB-like and the arc-like rocks (Figure 12). Note also that the initial ε_{Nd} values of low-grade Franciscan and the Feather River rocks were estimated at 130–195 Ma and 240 Ma, respectively, and yet they show distinct positive ε_{Nd} values in contrast with the present-day intra-oceanic arc data (Figure 12). Thus Nd-isotopic values are excellent indicators of protolith signatures, even at eclogite and garnet amphibolite facies of subduction metamorphism, implying little mobility of Sm and Nd during these high grades of metamorphism.

Actinolite rinds

Actinolite–chlorite–phengite rinds are locally present partly encasing many of the high-grade blocks in the Franciscan (Coleman and Lanphere 1971). In some rare cases where block–matrix relationships are exposed such blocks are enclosed in serpentinite matrix, and the rinds are also present between serpentinite selvages and coherent high-grade rocks (Wakabayashi and Dumitru 2007). The rinds have been interpreted to have formed as a result of metasomatic exchange between high-grade blocks and the enclosing ultramafic rocks (Coleman and Lanphere 1971;

Moore 1984). Three actinolite rind samples from the Ring Mountain locality (Figure 1) were analysed in our previous study (Saha *et al*. 2005). These data have been included in this study (Tables 1–4, Figures 1–12 1–12) to evaluate elemental mobility as these rocks clearly represent a very limited volume of the overall metamorphic material and are somewhat of a special case.

Geochemical results of actinolite rinds

Rinds show decrease in alkalis (Na_2O+K_2O) with increasing silica and are strikingly different from the rest of the rocks of this study that show a calc-alkaline trend (Figure 2). Rinds have slightly higher SiO_2 wt.% (46–51%), significantly higher MgO wt.% (13–20%) and Mg # (74–86), and variable low values of Al_2O_3 (16–3%), TiO_2 (0.45–0.05%), and low P_2O_5 (0.01%) wt.% relative to the rest of the Franciscan rocks (Figures 4 and 5). In all the major element variation diagrams (Figures 4 and 5), the actinolite rinds fall partially or completely outside the fields of the high- and low-grade Franciscan rocks.

Chondrite-normalized REE patterns for the actinolite rinds (Figure 6D) show low concentrations and flat LREE-depleted patterns. They plot below the field of the Pacific arc tholeiites and are unlike the REE patterns of the high- and low-grade Franciscan rocks and FRB. These rinds also lack any signature of continentally derived sediment as observed by the lack of any LREE enrichment (Figure 6D). In N-MORB-normalized trace element plots (Figure 7D), the rinds show high Ba and Pb concentrations similar to the high-grade rocks. In addition, they have high Ta and low La, Nb concentrations making their Nb–Ta pattern distinctly different from any of the arc or MORB-like rocks of this study.

High Ba/La ratio (Figure 8, Table 3), low Ce concentration (Figure 9), and high Th/La ratio (Figure 12) cause the rinds to fall distinctly away from other Franciscan and Feather River rocks. In a plot of Th/Nb versus La/Nb (Figure 10), the rinds fall in the field of either Kurile Arc or UCC. Presence of continental crust has already been eliminated for these rocks from their REE data (Figure 6D), and they differ geochemically from the other Franciscan and FRB rocks.

In their Pb-isotopic ratios (Figure 11), the rinds overlap with the Franciscan Pb data showing the lowest $^{207}Pb/^{204}Pb$ isotopic ratios, falling on the NHRL. This relationship confirms that no continental crustal Pb is present in these rinds.

Discussion of rind geochemistry

The rinds differ from the other rocks of this study in their major element composition with enriched MgO and SiO_2 wt.% and low Al_2O_3, TiO_2, and P_2O_5 wt.%, as well as differing in trace element composition. The absence of any continental crust-derived sediment during the metasomatism of these rinds is clear from their generally lower REE content and LREE depletion (Figure 6D) as well as low Pb-isotopic ratios plotting far removed from the UCC (EM II field; Figure 11). The low initial $\varepsilon_{Nd(I)}$ values (Table 4; Figure 12) of the actinolite rinds could be due to their sources being phosphates from fish debris or biogenic silica from bedded radiolarian chert (Shimizu *et al*. 2001) because the possibility of any old low ε_{Nd}-bearing continental component has already been eliminated on the basis of REE and Pb-isotopic data.

The combined geochemical data suggest that the rinds formed from depleted mantle-wedge ultramafic rock. They apparently experienced some metasomatism by fluids carrying Ba, Pb, and Sr from the upper part of the subducted slab. Although field relations imply that the high-grade metabasalts may have reacted with enclosing ultramafic rocks to form the rinds, geochemically there is no evidence of any reaction between the rinds and the metabasalts as the rinds have less enriched trace element concentrations and ratios (Figures 6–10 6–10) compared with the high- and low-grade Franciscan rocks. However, the high-grade rocks commonly include metacherts as well as metabasalts, so it is likely that fluids that interacted with ultramafic rocks to form the rinds were preferentially mobilized from metacherts that overlay or were intercalated with the metabasalts of the subducting slab.

FRB ultramafics and amphibolites

The FRB represents fragments of oceanic and sub-arc lithospheric mantle accreted to the western edge of North American Cordilleran collage during the Palaeozoic to early Mesozoic (Moores 1970; Schweickert and Snyder 1981; Smart and Wakabayashi 2009). Fluid-mobile elements (e.g. B, As, Li, Pb) in variably serpentinized harzburgite from the FRB have been analysed by Lee and co-workers (Agranier *et al*. 2007; Lee *et al*. 2008). These serpentinites are analogous to the mantle wedge that tectonically overlay the Franciscan Complex (but much older) and formed the rinds as discussed above. Based on major and trace element data, the FRB harzburgite protoliths have been suggested to be serpentinized under low water/rock ratio conditions and are representative of oceanic lithosphere mantle rather than abyssal peridotites. Fluid-mobile element concentrations of these serpentinites are due to low water/rock interaction during serpentinization rather than prograde metamorphism as indicated by their unradiogenic Os and near chondritic platinum group element sytematics (Agranier *et al*. 2007). This is consistent with the lack of elemental mobility in our FRB amphibolites, because if mobile elements had been expelled from these amphibolites due to subduction metamorphism, the overlying serpentinites would be expected to have been enriched in the most mobile elements.

Subduction-zone metamorphism elemental mobility: comparison with previous studies and insight into fluid migration pathways

Our conclusions of limited element mobility in subduction-zone metamorphism generally agree with those of some studies (Matthews and Schliestaedt 1984; Barnicoat and Cartwright 1995; Philippot *et al*. 1998; Scambelluri and Philippot 2001; Chalot-Prat *et al*. 2003; Scambelluri *et al*. 2004; Spandler *et al*. 2004), but differ markedly from some studies that advocated vastly more chemical mobility (e.g. Sorensen and Grossman 1989; Bebout and Barton 1993; Bebout *et al*. 1993; Bebout 1995; Sorensen *et al*. 1997; Arculus *et al*. 1999; Becker *et al*. 2000; Bebout 2007). Here we will discuss the details of the similarities and differences between our work and previous research and then speculate on possible fluid pathways in subduction-zone metamorphism.

Many studies advocating considerable elemental mobility in subduction-zone metamorphism were based primarily, but not entirely, on rocks from the Catalina schists of offshore California (e.g. Sorensen and Grossman 1989; Bebout and Barton 1993; Bebout *et al*. 1993; Bebout 1995; Sorensen *et al*. 1997; Bebout 2007). The Catalina schists have long been considered a metamorphic sole and subjacent subduction complex, analogous to the Franciscan Complex high-grade and lower grade rocks (e.g. Platt 1975) although the age of high-temperature metamorphism is about 50 million years younger for the Catalina schist (Mattinson 1986; Grove and Bebout 1995). Thus difference in data interpretation between these studies and ours appears puzzling indeed.

A possible resolution to this paradox may come from the recent study of Grove *et al.* (2008), who noted major contrasts in metamorphic age, metamorphic P–T paths, protolith types, and protolith ages, between the high-grade structurally high rocks of the Catalina schists and the high-grade rocks of the Franciscan. Grove *et al.* (2008) proposed that the structurally highest rocks of the Catalina schist represent continental arc basement and forearc basin deposits juxtaposed over lower grade (blueschist facies) typical subduction complex rocks by subduction erosion, rather than a metamorphic sole, formed at the initiation of subduction. According to this interpretation, the high-grade and low-grade rocks of the Catalina schists have dramatically different protoliths, igneous, and metamorphic histories, and the difference in chemistry between them cannot be explained by progressive metamorphism of subducted oceanic basalts and trench sediments. Thus, we believe that much of the difference in chemistry between Catalina schist rocks of different metamorphic grades reflects differences in protoliths and igneous and metamorphic histories instead of chemical modification associated with progressive metamorphism of the same protoliths.

Sorensen *et al.* (1997) examined major and trace element chemistry of subduction-zone metamorphic rocks from the Franciscan (low-grade and high-grade blocks) and Samana Peninsula of the Dominican Republic and concluded that the geochemistry of these rocks indicated enrichment in K, Ba, Rb, and Cs by subduction-zone fluids and melts. Although they considered a difference in protolith type between Franciscan (interpreted as MORB affinity) and Samana Peninsula (interpreted as island-arc basalt affinity), they interpreted the chemistry of Franciscan rocks as a product of metamorphic modification of a common MORB protolith, in contrast to our identification of different protolith types in Franciscan metabasalts. Their conclusion of enrichment of LILE during metamorphism is similar to our conclusions for higher grade rocks, but their interpretation that the enrichment is a result of interaction with fluids from metasediment is contrary to our evidence of a lack of sediment signature and it is also contrary to multiple studies conducted on rocks up to eclogite grade that show preservation of small-scale (centimetre- and millimetre-scale) protolith heterogeneity with associated small-scale closed-system chemical behaviour (Matthews and Schliestaedt 1984; Barnicoat and Cartwright 1995; Philippot *et al*. 1998; Scambelluri and Philippot 2001; Chalot-Prat *et al*. 2003; Scambelluri *et al*. 2004).

Other studies have advocated large-scale chemical modification during subduction metamorphism (e.g. Arculus *et al*. 1999; Becker *et al*. 2000) and both of these studies reached their conclusions based on an assumed common protolith composition. In the opinion of Spandler *et al.* (2004), with which we concur, the interpreted chemical modification is an artefact of protolith differences that were not considered in those studies.

Published studies advocating minimal elemental mobility have much in common with our conclusions, but there are some differences that are important in evaluating general subduction-zone fluid pathways. A number of studies, focused primarily on rocks of the Alpine region, used stable isotopic data to show a lack of chemical exchange and chemical alteration of subducted rocks during metamorphism up to HP and ultrahigh-pressure (UHP) eclogite grade (Matthews and Schliestaedt 1984; Getty and Selverstone 1994; Barnicoat and Cartwright 1995; Philippot *et al*. 1998). Of these works, Philippot *et al.* (1998) included evaluation of Franciscan Complex data. Busignya *et al.* (2003) reached similar conclusions using both stable isotopic data and K, Rb, and Cs concentrations. Matthews and Schliestaedt (1984) noted significant chemical modification associated with greenschist overprinting of blueschists. The tectonothermal history of those rocks (Sifnos, Cyclades) differs from the Franciscan in that the latter lacks a thermal overprint owing to syn-subduction exhumation under conditions of low geothermal gradient (e.g. Ernst 1988).

Chalot-Prat *et al.* (2003) examined major and trace element as well as radiogenic isotopic data from eclogites and

associated ultramafic rocks in the Western Alps and concluded virtually no element mobility during metamorphism based on comparison of compositional data to unmetamorphosed rocks interpreted as protolith equivalents. Using major and trace element data from blueschists, eclogites, and garnet amphibolites from New Caledonia, Spandler *et al.* (2004) concluded that chemical modification during subduction metamorphism was minor and vastly subordinate to chemical variation in the original protoliths. They proposed that three of their samples show LILE depletion that might be associated with the release of these fluids to the overlying mantle.

Our interpretations of element mobility during subduction metamorphism are similar to previous studies that have advocated minimal chemical modification during subduction metamorphism, but we differ in that we believe our data show an increasing amount of enrichment in some elements, such as Ba and Pb, with increasing metamorphic grade (e.g. Figures 8 and 9). In addition, we show spatially limited chemical modification of mantle in contact with metamorphic rocks that resulted from interaction with fluids that were preferentially mobilized from metachert rather than the volumetrically more significant metabasalt. The trend of increasing Ba and Pb enrichment with increasing metamorphic grade in MORB coupled with the lack of evidence of sediment input indicates that Ba and Pb are lost from the basaltic slab somewhere down-dip (at higher grade) than the region of metamorphism of our samples. Our rind data suggest that the fluids hydrating the mantle above the subducting slab to the maximum depth of metamorphism recorded in our samples (ca. 70 km for eclogites) are derived from metachert, not metabasalt, so the Ba and Pb depleted at higher grade from metabasalt migrated up-dip in the slab but reacted preferentially with the highest grade rocks that would represent the shortest transport distance from their point of depletion. One of our high-grade Franciscan sample shows depletion in Pb and Ba (Figure 7A). This sample may have reached the point where it released Ba- and Pb-rich fluid. This sample may be analogous to the three samples in Spandler *et al.* (2004) that showed LILE depletion.

The conclusion of limited chemical mobility in subduction metamorphism appears difficult to reconcile with the data of Mottl *et al.* (2004), who showed a systematic change with distance from the trench in the chemistry of cold springs in serpentinite mud volcanoes in the Marianas forearc. These authors attributed this change to fluids liberated at increasing temperature and depth from the sediments or altered basalt atop the subducting plate. Based on the collective data from our metabasalts and rinds, we believe that chemical data from the Marianas is compatible with a model in which fluids are preferentially liberated from sediments on the top of the basaltic crust, which in an environment such as the Marianas, or the early Franciscan trench, are pelagic sediments (chert in the case of the Franciscan). Although fluids derived from subducted chert interacted with and chemically modified the mantle above the subduction zone, they did not interact with basalt of the subducting slab.

Conclusions

We have shown that element mobility in subduction-zone metamorphism must be evaluated by simultaneous consideration of potential chemical differences in protoliths as well as elemental exchange and fractionation during metamorphic processes. This conclusion echoes that of Spandler *et al.* (2004), who studied similar HP metamorphic rocks from New Caledonia. We hypothesize that studies that have concluded significant chemical modification by subduction metamorphism did so by not adequately accounting for the chemical variability of different protoliths that were subducted. Our conclusion of limited chemical mobility in subduction metamorphism is supported by numerous previous studies on a variety of localities of HP and UHP rocks involving stable isotopic data (e.g. Matthews and Schliestaedt 1984; Getty and Selverstone 1994; Barnicoat and Cartwright 1995; Philippot *et al*. 1998) as well as major and trace element and radiogenic isotope data (Chalot-Prat *et al*. 2003; Spandler *et al*. 2004). Although our conclusions are similar to these prior studies, we do show preferential mobilization of fluids from subducted metachert as well as mobilization of Ba and Pb within the subducted metabasalt slab. This suggests that the hydration and chemical modification of the forearc mantle up-dip of the region of arc magmatism is largely driven by release of fluids from subducted sediment rather than from basalt. The silica depletion noted in some of our rocks is apparently a consequence of seafloor alteration, rather than subduction metamorphism, consistent with the conclusions of Philippot *et al.* (1998).

Our data show the lack of chemical interaction with subducted sediment, even though large-scale clastic sediment subduction accretion occurred before or synchronous with the subduction of several of our samples. This result is consistent with the conclusions of studies that showed the lack of chemical exchange, even between very fine scale compositional layering in subducted rocks up to eclogite grade (e.g. Matthews and Schliestaedt 1984; Getty and Selverstone 1994; Barnicoat and Cartwright 1995; Philippot *et al*. 1998).

In concurrence with previous studies that have argued for minimal chemical mobility in the subducted slab to the depth of arc magmatism, we regard our data as showing that significant element exchange does not occur until the ultimate breakdown of hydrous minerals such as calcic amphibole, phengite, and epidote – the common hydrous minerals in the highest grade metabasalts of our study. Hermann and Green (2001) concluded on the basis of their

experiments that the breakdown of phengite has the greatest influence in chemical exchange at the depth of arc magma genesis. However, the bulk composition used in their experiments is more representative of subducted sediments rather than subducted basalt. For rocks of basaltic composition, Ca-amphibole is likely to play a large role along with phengite and possibly epidote, owing to its abundance in higher grade subduction-zone metabasaltic rocks (Ernst 1999).

Acknowledgements

This research was supported by a National Science Foundation grant EAR-0635767 (awarded to A.R.B and J.W). We thank Dr L. Reisberg, K. Simons, and H. Zou for critical comments and suggestions that improved this manuscript.

References

Agranier, A., Lee, C.-T.A., Li, Z.-X.A., and Leeman, W.P., 2007, Fluid mobile element budgets in serpentinized oceanic lithospheric mantle: Insights from B, As, Li, Pb, PGEs and Os isotopes in the Feather River Ophiolite, California: Chemical Geology, v. 245, p. 230–241.

Anczkiewicz, R., Platt, J.P., Thirlwall, M.F., and Wakabayashi, J., 2004, Franciscan subduction off to a slow start: Evidence from high-precision Lu-Hf garnet ages on high grade-blocks: Earth and Planetary Science Letters, v. 225, p. 147–161.

Arculus, R.J., Lapierre, H., and Jaillard, E., 1999, Geochemical window into subduction and accretion processes; Raspas metamorphic complex, Ecuador: Geology, v. 27, p. 547–550.

Arnórsson, S., 1970, Geochemical studies of thermal waters in the Southern Lowlands of Iceland: Geothermics, Special Issue, v. 2, p. 547–552.

Bailey, E.H., Irwin, W.P., and Jones, D.L., 1964, Franciscan and related rocks, and their significance in the geology of western California: California Division of Mines and Geology Bulletin, v. 183, 171 p.

Barnicoat, A.C., and Cartwright, I., 1995, Focused fluid flow during subduction: Oxygen isotope data from high-pressure ophiolites of the western Alps: Earth and Planetary Science Letters, v. 132, p. 53–61.

Basu, A.R., Sharma, M., and DeCelles, P.G., 1990, Nd, Sr-isotopic provenance and trace element geochemistry of Amazonian foreland basin fluvial sands, Bolivia and Peru; implications for ensialic Andean Orogeny: Earth and Planetary Science Letters, v. 100, p. 1–17.

Bebout, G.E., 1995, The impact of subduction-zone metamorphism on mantle-ocean chemical cycling: Chemical Geology, v. 126, p. 191–218.

Bebout, G.E., 2007, Metamorphic chemical geodynamics of subduction zones: Earth and Planetary Science Letters, v. 260, p. 373–393.

Bebout, G.E., and Barton, M.D., 1993, Metasomatism during subduction: Products and possible paths in the Catalina Schist, California: Chemical Geology, v. 108, p. 61–92.

Bebout, G.E., Ryan, J.G., Leeman, W.P., and Bebout, A.E., 1993, Fractionation of trace element and stable isotope signatures during subduction-zone metamorphism: EOS (Transactions of the American Geophysical Union), v. 74, p. 331.

Becker, H., Jochum, K.P., and Carlson, R.W., 2000, Trace element fractionation during dehydration of eclogites from high-pressure terranes and the implication for element fluxes in subduction zones: Chemical Geology, v. 163, p. 65–99.

Blake, M.C., Jayko, A.S., McLaughlin, R.J., and Underwood, M.B., 1988, Metamorphic and tectonic evolution of the Franciscan Complex, northern California, in Ernst, W.G., ed., *Metamorphism and crustal evolution of the western United States, Rubey Volume 7: Englewood Cliffs, New Jersey*, Prentice-Hall, p. 1035–1060.

Bottinga, Y., 1969, Calculated fractionation factors for carbon and hydrogen isotope exchange in the system calcite-carbon dioxide-graphite-methane-hydrogen-water vapor: Geochimica et Cosmochimica Acta, v. 33, p. 49–64.

Böhlke, J.K., and McKee, E.H., 1984, K-Ar ages relating to metamorphism, plutonism, and gold-quartz vein mineralization near Alleghany, Sierra County, California: Isochron/West, v. 39, p. 3–7.

Bowers, S.T., Vondamm, K.L., and Edmond, J.M., 1985, Chemical evolution of mid-ocean ridge hot springs: Geochimica et Cosmochimica Acta, v. 49, p. 2239–2252.

Brown, E.H., and Ghent, E.D., 1983, Mineralogy and phase relations in the blueschist facies of the Black Butte and Ball Rock areas, northern California Coast Ranges: American Mineralogist, v. 68, p. 365–372.

Busignya, V., Cartigny, P., Philippot, P., Ader, M., and Javoy, M., 2003, Massive recycling of nitrogen and other fluid-mobile elements (K, Rb, Cs, H) in a cold slab environment: Evidence from HP to UHP oceanic metasediments of the schistes Lustre´s nappe (western Alps, Europe): Earth and Planetary Science Letters, v. 215, p. 27–42.

Carmichael, I.S.E., Turner, F.J., and Verhoogen, J., 1974, Igneous Petrology: New York, McGraw Hill.

Chacko, T., Mayeda, T.K., Clayton, R.N., and Goldsmith, J.R., 1991, Oxygen and carbon isotope fractionation between CO_2 and calcite: Geochimica et Cosmochimica Acta, v. 55, p. 2867–2882.

Chalot-Prat, F., Ganne, J., and Lombard, A., 2003, No significant element transfer from the oceanic plate to the mantle wedge during subduction and exhumation of the Tethys lithosphere (Western Alps): Lithos, v. 69, p. 69–103.

Church, S.E., and Tatsumoto, M., 1975, Lead isotope relations in oceanic ridge basalts from the Juan de Fuca-Gorda Ridge Area, N.E. Pacific Ocean: Contributions to Mineralogy and Petrology, v. 53, p. 253–279.

Coleman, R.G., and Lanphere, M.A., 1971, Distribution and age of high-grade blueschists, associated eclogites, and amphibolites from Oregon and California: Geological Society of America Bulletin, v. 82, p. 2397–2412.

Dickens, A.P., 1995, Radiogenic isotopes geology: New York, Cambridge University Press.

Dickinson, W.R., 1970, Relations of andesites, granites and derivative sandstones to arc-trench tectonics: Reviews of Geophysics and Space Physics, v. 8, p. 813–860.

Dumitru, T.A., Wakabayashi, J., Wright, J.E., and Wooden, J.L., 2010, Early Cretaceous (ca. 123 Ma) transition from nonaccretion to voluminous sediment accretion within the Franciscan subduction complex: Tectonics, v. 29, TC5001 p.

Edelman, S.H., Day, H.W., Moores, E.M., Zigan, S.M., Murphy, T.P., and Hacker, B.P., 1989, Structure across a Mesozoic ocean-continent suture zone in the northern Sierra Nevada, California: Geological Society of America. Special Paper, v. 224, p. 55.

Edelman, S.H., and Sharp, W.D., 1989, Terranes, early faults, and pre-Late Jurassic amalgamation of the western Sierra Nevada metamorphic belt, California: Geological Society of America Bulletin, v. 101, p. 1420–1433.

Ehrenberg, S.N., 1975, Feather River Ultramafic Body, Northern Sierra Nevada, California: Geological Society of America Bulletin, v. 86, p. 1235–1243.

Elliott, T., Plank, T., Zindler, A., White, W., and Bourdon, B., 1997, Element transport from slab to volcanic front at the Mariana arc: Journal of Geophysical Research, v. 102, p. 14991–15019.

Erickson, R.C., Mattinson, J., Dumitru, T.A., and Sharp, W.D., 2004, Petrology, isotope geochemistry, and geochronology of a multiply-metamorphosed granitoid exotic block in a Franciscan olistostrome mélange, Cazadero, California: Geological Society of America Abstracts with Programs, v. 36, p. 39.

Ernst, W.G., 1970, Tectonic contact between the Franciscan mélange and the Great Valley Sequence, crustal expression of a Late Mesozoic Benioff Zone: Journal of Geophysical Research, v. 75, p. 886–902.

Ernst, W.G., 1971, Do mineral parageneses reflects unusually high-pressure conditions of Franciscan metamorphism?: American Journal of Science, v. 270, p. 81–108.

Ernst, W.G., 1988, Tectonic history of subduction zones inferred from retrograde blueschist P-T paths: Geology, v. 16, p. 1081–1084.

Ernst, W.G., 1993, Metamorphism of Franciscan tectonostratigraphic assemblage, Pacheco Pass area, east-central Diablo Range, California Coast Ranges: Geological Society of America Bulletin, v. 105, p. 618–636.

Ernst, W.G., 1999, Hornblende, the continent maker – Evolution of H_2O during circum-Pacific subduction versus continental collision: Geology, v. 27, p. 675–678.

GEOROC database. http://georoc.mpch-mainz.gwdg.de/Entry.html

Getty, S.R., and Selverstone, J., 1994, Stable isotopic and trace element evidence for restricted fluid migration in 2 GPa eclogites: Journal of Metamorphic Geology, v. 12, p. 747–760.

Giaramita, M., MacPherson, G.J., and Phipps, S.P., 1998, Petrologically diverse basalts from a fossil oceanic fore arc in California: The Llanada and Black Mountain remnants of the Coast Range Ophiolite: Geological Society of America Bulletin, v. 110, p. 553–571.

Grove, M., and Bebout, G.E., 1995, Cretaceous tectonic evolution of coastal southern California: Insights from the Catalina Schist: Tectonics, v. 14, p. 1290–1308.

Grove, M., Bebout, G.E., Jacobson, C.E., Barth, A.P., Kimbrough, D.L., King, R.L., Zou, H., Lovera, O.M., Mahoney, B.J., and Gehrels, G.G., 2008, The Catalina schist: Evidence for middle Cretaceous subduction erosion of southwestern North America, in Draut, A.E., Clift, P.D., and Scholl, D.W., eds., Formation and applications of the sedimentary record in arc collision zones: Geological Society of America Special Paper. 436, p. 335–362.

Hamilton, W.B., 1969, Mesozoic California and underflow of the Pacific Mantle: Geological Society of America Bulletin, v. 80, p. 2409–2430.

Hanan, B.B., and Schilling, J.-G., 1989, Easter microplate evolution: Pb isotope evidence: Journal of Geophysical Research, v. 94, p. 7432–7448.

Hart, S.R., and Staudigel, H., 1989, Isotopic characterization and identification of recycled components, in Hart, S.R., and Gulen, L., eds., Crust mantle recycling at convergence zones: Dordrecht/Boston, Massachusetts, D. Reidel Publishing Company, p. 15–28.

Hawkesworth, C.J., O'Nions, R.K., Pankhurst, R.J., Hamilton, P.J., and Evensen, N.M., 1977, A geochemical study of island-arc and back-arc tholeiites from the Scotia Sea: Earth and Planetary Science Letters, v. 36, p. 253–262.

Hermann, J., and Green, D.H., 2001, Experimental constraints on high pressure melting in subducted crust: Earth and Planetary Science Letters, v. 188, p. 149–168.

Hietanen, A., 1981, Geology west of the Melones fault between the Feather River and North Yuba Rivers, California. U.S. Geological Survey Professional Paper 1226-A, 25 p.

Hofmann, A.W., Jochum, K.P., and White, W.M., 1986, Nb and Pb in oceanic basalts: New constraints on mantle evolution: Earth and Planetary Science Letters, v. 79, p. 33–45.

Hopson, C.A., Mattinson, J.M., and Pessagno, E.A., Jr., 1981, Coast Range Ophiolite, western California, in Ernst, W.G., Geotectonic Development of California: Englewood Cliffs, New Jersey, Prentice-Hall, p. 418–510.

Hopson, C.A., Mattinson., J.M., Pessagno, E.A., Jr., and Luyendyk, B.P., 2008, California coast range ophiolite: Composite Middle and Late Jurassic oceanic lithosphere, in Wright, J.E., and Shervais, J.W., eds., Ophiolites, arcs, and batholiths: A tribute to Cliff Hopson. Geological Society of America Special Paper 483, p. 1–101.

Hsü, K.J., 1968, The principles of melanges and their bearing on the Franciscan-Knoxville paradox: Geological Society of America Bulletin, v. 79, p. 1063–1074.

Jacobsen, S.B., and Wasserburg, G.J., 1984, Sm-Nd isotopic evolution of chondrites and achondrites, II: Earth Planetary Science Letters, v. 67, p. 137–150.

Jakes, P., and Gill, J., 1970, Rare Earth Elements and the Island Arc Tholeiitic Series: Earth and Planetary Science Letters, v. 9, p. 17–28.

Kay, W., 1978, Aleutian magnesian andesites: Melts from subducted Pacific Ocean crust: Journal of Volcanological and Geothermal Research, v. 4, p. 117–132.

Kent, A.J.R., and Elliott, T.R., 2002, Melt inclusions from Marianas arc lavas: Implications for the composition and formation of island arc magmas: Chemical Geology, v. 183, p. 263–286.

Krogh, E.J., Oh, C.W., and Liou, J.G., 1994, Polyphase and anticlockwise P-T evolution for Franciscan eclogites and blueschists from Jenner, California, USA: Journal of Metamorphic Geology, v. 12, p. 121–134.

Lee, C.-T.A., Oka, M., Luffi, P., and Agranier, A., 2008, Internal distribution of Li and B in serpentinites from the Feather River Ophiolite, California, based on laser ablation inductively coupled plasma mass spectrometry: Geochemistry Geophysics Geosystems, v. 9, p. Q12011.

Leeman, W.P., Carr, M.J., and Morris, J.D., 1994, Boron geochemistry of the Central American Volcanic Arc: Constraints on the genesis of subduction-related magmas: Geochimica et Cosmochimica Acta, v. 58, p. 149.

Lofgren, G.E., Grove, T.L., Brown, R.W., and Smith, D.P., 1979, Comparison of dynamic crystallization techniques on Apollo 15 quartz normative basalts: Proceedings of the Lunar and Planetary Science Conference, v. 10, p. 423–438.

MacPherson, G.J., 1983, The Snow Mountain complex: An on-land seamount in the Franciscan terrain, California: Journal of Geology, v. 91, p. 73–92.

MacPherson, G.J., Phipps, S.P., and Grossman, J.N., 1990, Diverse sources for igneous blocks in Franciscan melanges, California Coast Ranges: Journal of Geology, v. 98, p. 845–862.

Magaritz, M., and Taylor, H.P., Jr., 1976, Oxygen, hydrogen and carbon isotope studies of the Franciscan formation, Coast Ranges, California: Geochimica et Cosmochimica Acta, v. 40, p. 215–234.

Maruyama, S., and Liou, J.G., 1988, Petrology of Franciscan metabasites along the jadeite-glaucophane type facies series, Cazadero, California: Journal of Petrology, v. 29, p. 1–37.

Maruyama, S., Liou, J.G., and Sasakura, Y., 1985, Low-temperature recrystallization of Franciscan greywackes from Pacheco Pass, California: Mineralogical Magazine, v. 49, p. 345–355.

Matthews, A., and Schliestedt, M., 1984, Evolution of the blueschist and greenschist facies rocks of Sifnos, Cyclades Greece: A stable isotope study of subduction-related metamorphism: Contributions to Mineralogy and Petrology, v. 88, p. 150–163.

Mattinson, J.M., 1986, Geochronology of high-pressure-low-temperature Franciscan metabasites: A new approach using the U-Pb system, in Evans, B.W., and Brown, E.H., eds., Blueschists and eclogites: Geological Society of America Memoir 164, p. 95–106.

Meijer, A., 1976, Pb and Sr isotopic data bearing on the origin of volcanic rocks from the Mariana island-arc system: Geological Society of America Bulletin, v. 87, p. 1358–1369.

Moore, D.E., 1984, Metamorphic history of a high-grade blueschist exotic block from the Franciscan Complex, California: Journal of Petrology, v. 25, p. 126–150.

Moores, E.M., 1970, Ultramafics and orogeny, with models of the US Cordillera and the Tethys: Nature, v. 228, p. 837–842.

Moran, A.E., Sisson, V.B., and Leeman, W.P., 1992, Boron depletion during progressive metamorphism: Implications for subduction processes: Earth and Planetary Science Letters, v. 111, p. 331–349.

Mottle, M.J., Wheat, C.G., Fryer, P., Gharib, J., and Martin, J.B., 2004, Chemistry of springs across the Mariana forease shows progressive devolatization of the subducting slab: GLA, v. 68, p. 4915–4933.

Murton, B.J., Peate, D.W., Arculus, R.J., Pearce, J.A., and van der Laan, S., 1992, Trace-element geochemistry of volcanic rocks from Site 786: The Izu-Bonin forearc, in Fryer, P., Pearce, J.A., and Stokking, L.B., eds., Proceedings of the Ocean Drilling Program Scientific Results 125, College Station, Texas (Ocean Drilling Program), p. 211–235.

Nakamura, K., Kato, Y., Tamaki, K., and Ishii, T., 2007, Geochemistry of hydrothermally altered basaltic rocks from the Southwest Indian Ridge near the Rodriguez Triple Junction: Marine Geology, v. 239, p. 125–141.

Nelson, B.K., 1991, Sediment-derived fluids in subduction zones; isotopic evidence from veins in blueschist and eclogite of the Franciscan Complex, California: Geology, v. 19, p. 1033–1036.

Nelson, B.K., 1995, Fluid flow in subduction zones; evidence from Nd- and Sr-isotope variations in metabasalts of the Franciscan Complex, California: Contributions to Mineralogy and Petrology, v. 119, p. 247–262.

Nelson, B.K., and DePaolo, D.J., 1985, Isotopic investigation of metamorphism in subduction zones; the Franciscan Complex, California: Abstracts with Programs – Geological Society of America, v. 17, p. 674–675.

Page, F.Z., Armstrong, L.S., Essene, E.J., and Mukasa, S.B., 2007, Prograde and retrograde history of the Junction School eclogite, California, and an evaluation of garnet-phengite-clinopyroxene thermobarometry: Contributions of Mineralogy and Petrology, v. 153, p. 533–555.

Pearce, J.A., van der Laan, S.R., Arculus, R.J., Murton, B.J., Ishii, T., Peate, D.W., and Parkinson, I.J., 1992, Boninite and Harzburgite from Leg 125 (Bonin-Mariana forearc): A case study of magma genesis during the initial stages of subduction, in Fryer, P., Pearce, J., and Stokking, L.B., eds., Proceedings of the ocean Drilling Program Scientific results 125 (Ocean Drilling Program), Texas, p. 623–659.

Pearson, N.J., O'Reilly, S.Y., and Griffin, W.L., 1991, Heterogeneity in the thermal state of the lower crust beneath eastern Australia: Exploration Geoscience, v. 22, p. 295–298.

Philippot, P., Agrinier, P., and Scambelluri, M., 1998, Chlorine cycling in the subducted oceanic lithosphere: Earth and Planetary Science Letters, v. 161, p. 33–44.

Plank, T., 2005, Constraints from thorium/lanthanum on sediment recycling at subduction zones and the evolution of the continents: Journal of Petrology, v. 46, p.921–944.

Plank, T., and Langmuir, C.H., 1998, The chemical composition of subduction sediments and its consequences for the crust and mantle: Chemical Geology, v. 145, p. 325–394.

Platt, J.P., 1975, Metamorphic and deformational processes in the Franciscan Complex, California: Some insights from the Catalina Schist terrain: Geological Society of America Bulletin, v. 86, p. 1337–1347.

Platt, J.P., 1986, Dynamics of orogenic wedges and the uplift of high-pressure metamorphic rocks: Geological Society of America Bulletin, v. 97, p. 1037–1053.

Ridley, W.I., Perfit, M.R., Jonasson, I.R., and Smith, M.F., 1994, Hydrothermal alteration in oceanic ridge volcanics; a detailed study at the Galapagos fossil hydrothermal field: Geochimica et Cosmochimica Acta, v. 58, p. 2477–2494.

Ross, J.A., and Sharp, W.D., 1986, $^{40}Ar/^{39}Ar$ and Sm/Nd dating of garnet amphibolite in the Coast Ranges, California: EOS (Transactions of the American Geophysical Union), v. 67, p. 1249.

Ross, J.A., and Sharp, W.D., 1988, The effects of sub-blocking temperature metamorphism on the K/Ar systematics of hornblendes: $^{40}Ar/^{39}Ar$ dating of polymetamorphic garnet amphibolite from the Franciscan Complex, California: Contributions to Mineralogy and Petrology, v. 100, p. 213–221.

Ryan, J.G., and Langmuir, C.H., 1993, The systematics of boron abundances in young volcanic rocks: Geochimica et Cosmochimica Acta, v. 57, p. 1489–1498.

Saha, A., Basu, A.R., Wakabayashi, J., and Wortman, G.L., 2005, Geochemical evidence for subducted nascent arc from Franciscan high-grade tectonic blocks: Geological Society of America Bulletin, v. 117, p. 1318–1335.

Saleeby, J.B., Shaw, H.F., Niemeyer, S., Moores, E.M., and Edelman, S.H., 1989, U/Pb, Sm/Nd and Rb/Sr geochronological and isotopic study of Northern Sierra Nevada ophiolitic assemblages, California: Contributions to Mineralogy and Petrology, v. 102, p. 205–220.

Scambelluri, M., Fiebig, J., Malaspina, N., Muentener, O., and Pettke, T., 2004, Serpentinite subduction: Implications for fluid processes and trace-element recycling: International Geology Review, v. 46, p. 595–613.

Scambelluri, M., and Philippot, P., 2001, Deep fluids in subduction zones: Lithos, v. 55, p. 213–227.

Schweickert., R.A., and Snyder, W.S., 1981, Paleozoic plate tectonics of the Sierra Nevada and adjacent regions, in Ernst, W.G., ed., Geotectonic Development of California Rubey Volume I: Englewood Cliffs, New Jersey, Prentice-Hall, p. 182–202.

Sharma, M., Basu, A.R., and Nesterenko, G.V., 1992, Temporal Sr-, Nd-, and Pb-isotopic variations in the Siberian flood basalts; implications for the plume-source characteristics: Earth and Planetary Science Letters, v. 113, p. 365–381.

Sharp, W., 1988, Pre-Cretaceous crustal evolution of the Sierra Nevada region, California, in Ernst, W.G., ed., Metamorphism and crustal evolution of the western United States, Rubey Volume VII: Englewood Cliffs, New Jersey, Prentice-Hall, p. 824–864.

Shervais, J.W., 1990, Island arc and ocean crust ophiolites; contrasts in the petrology, geochemistry and tectonic style of ophiolite assemblages in the California Coast Ranges, in Malpas, J., Moores, E., Panayiotou, A., and Xenophontos, C., eds., Ophiolites oceanic crustal analogues: Proceedings of the Symposium 'Troodos 1987', Nicosia, Cyprus, Geological Survey Department, Ministry of Agriculture and Natural Resources, p. 507–520.

Shervais, J.W., 2001, Birth, death, and resurrection: The life cycle of supra subduction zone ophiolites: Geochemistry, Geophysics, Geosystems, v. 2, 2000GC000080.

Shervais, J.W., Choi, S.H., Sharp, W.D., Ross, J., Zoglman-Schuman, M., and Mukasa, S., 2011, Serpentinite matrix mélange: Implications of mixed provenance for mélange formation, in Wakabayashi, J., and Dilek, Y., eds., Mélanges: Process of formation and societal significance. Geological Society of America Special Paper (in press).

Shervais, J.W., and Kimbrough, D.L., 1987, Alkaline and transitional subalkaline metabasalts in the Franciscan Complex mélange, California, in Morris, E.M., and Pasteris, J.D., eds., South-central Section meeting on alkalic rocks and kimberlites, Geological Society of America, p. 165–182.

Shervais, J.W., Murchey, B.L., Kimbrough, D.L., Renne, P.R., and Hanan, B., 2005, Radioisotopic and biostratigraphic age relations in the Coast Range ophiolite, northern California: Implications for the tectonic evolution of the western Cordillera: Geological Society of America Bulletin, v. 117, p. 633–653.

Shibakusa, H., and Maekawa, H., 1997, Lawsonite-bearing eclogitic metabasites in the Cazadero area, northern California: Mineralogy and Petrology, v. 61, p. 163–180.

Shimizu, H., Kunimaru, T., Yoneda, S., and Adachi, M., 2001, Source and depositional environments of some Permian and Triassic cherts; significance of Rb-Sr and Sm-Nd isotopic and REE abundance data: Journal of Geology, v. 109, p. 105–125.

Smart, C.M., and Wakabayashi, J., 2009, Hot and deep: Rock record of subduction initiation and exhumation of high-temperature, high-pressure metamorphic rocks, Feather River ultramafic belt, California: Lithos, doi: 10.1016/j.lithos.2009.06.012.

Snow, C.A., Wakabayashi, J., Ernst, W.G., and Wooden, J.L., 2010, SHRIMP-based depositional ages of Franciscan metagraywackes, west-central California: Geological Society of America Bulletin, v. 122, p. 282–291.

Sorensen, S.S., and Grossman, J.N., 1989, Enrichment of trace elements in garnet amphibolites from a paleo-subduction zone: Catalina Schist, southern California: Geochimica et Cosmochimica Acta, v. 53, p. 3155–3177.

Sorensen, S.S., Grossman, J.N., and Perfit, M.R., 1997, Phengite-hosted LILE enrichment in eclogite and related rocks: Implications for fluid-mediated mass transfer in subduction zones and arc magma genesis: Journal of Petrology, v. 38, p. 3–34.

Spandler, C., Hermann, J., Arculus, R., and Mavrogenes, J., 2004, Geochemical heterogeneity and element mobility in deeply subducted oceanic crust; insights from high-pressure mafic rocks from New Caledonia: Chemical Geology, v. 206, p. 21–42.

Stern, R.J., and Bloomer, S.H., 1992, Subduction zone-infancy: Examples from the Eocene Izu-Bonin-Mariana and Jurassic California arcs: Geological Society of America Bulletin, v. 1041, p. 1621–1636.

Sun, S.-S., and McDonough, W.F., 1989, Chemical and isotopic systematics of oceanic basalts: Implications for mantle composition and processes. Magmatism in the ocean basins. Geological Society Special Publication 42, p. 313–345.

Surpless, K.D., Graham, S.A., Covault, J.A., and Wooden, J.L., 2006, Does the Great Valley Group contain Jurassic strata? Reevaluation of the age and early evolution of a classic forearc basin: Geology, v. 34, p. 21–24.

Tatsumi, Y., and Eggins, S., 1995, Subduction Zone Magmatism: Oxford, United Kingdom, Blackwell, 211 p.

Tatsumoto, M., 1978, Isotopic composition of lead in oceanic basalts and its implications to mantle evolution: Earth and Planetary Science Letters, v. 38, p. 63–87.

Taylor, B.E., 1986, Magmatic volatiles: Isotopic variation of C, H, and S, in *Valley, J.W., Taylor, H.P., Jr., and O'Neil, J.R., eds., Stable isotopes in high temperature geological processes: Mineralogical Society of America*, v. 16, p. 185–225.

Taylor, H.P., and Coleman, R.G., 1968, $^{18}O/^{16}O$ ratios of coexisting minerals in glaucophane bearing metamorphic rocks: Geological Society of America Bulletin, v. 79, p. 1727–1756.

Taylor, S.R., and McLennan, S.M., 1985, The geochemical evolution of the continental crust: Reviews of Geophysics, v. 33, 241–265 p.

Tsujimori, T., Matsumoto, K., Wakabayashi, J., and Liou, J.G., 2006a, Franciscan eclogite revisited: Reevaluation of P-T evolution of tectonic blocks from Tiburon Peninsula, California, USA: Mineralogy and Petrology, v. 88, p. 243–267.

Tsujimori, T., Sisson, V.B., Liou, J.G., Harlow, G.E., and Sorensen, S.S., 2006b, Very-low-temperature record of the subduction process: A review of worldwide lawsonite eclogites: Lithos, v. 92, p. 609–624.

VonDamn, K.L., Edmond, J.M., Grant, B., Measures, C.I., Walden, B., and Weiss, R.F., 1985, Chemistry of submarine hydrothermal solutions at 218N, East Pacific Rise: Geochimica et Cosmochimica Acta, v. 49, p. 2197–2220.

Wakabayashi, J., 1987, Amphibolite grade metamorphism of Franciscan rocks from the San Francisco Bay Area, California: Geological Society of America Abstracts with Programs, v. 19, p. 460.

Wakabayashi, J., 1990, Counterclockwise P-T-t paths from amphibolites, Franciscan Complex, California: Relics from the early stages of subduction zone metamorphism: Journal of Geology, v. 98, p. 657–680.

Wakabayashi, J., 1992, Nappes, tectonics of oblique plate convergence, and metamorphic evolution related to 140 million years of continuous subduction, Franciscan Complex, California: Journal of Geology, v. 100, p. 19–40.

Wakabayashi, J., 1999, Subduction and the rock record: Concepts developed in the Franciscan Complex, California, in Sloan, D., Moores, E.M., and Stout, D., eds., Classic cordilleran concepts: A view from California. Geological Society of America Special Publication, p. 123–133.

Wakabayashi, J., and Deino, A.1989, Laser-probe $^{40}Ar/^{39}Ar$ ages from high grade blocks and coherent blueschists, Franciscan Complex, California: Preliminary results and implications for Franciscan tectonics: Geological Society of America Abstracts with Programs, v. 21, p. A267.

Wakabayashi, J., and Dumitru, T.A., 2007, $^{40}Ar/^{39}Ar$ ages from coherent high-pressure metamorphic rocks of the Franciscan Complex, California: Revisiting the timing of

metamorphism of the world's type subduction complex: International Geology Review, v. 49, p. 873–906.
Wakabayashi, J., Ghatak, A., and Basu, A.R., 2010, Tectonic setting of supra subduction zone ophiolite generation and subduction initiation as revealed through geochemistry and regional field relationships: Geological Society of America Bulletin, v. 122, p. 1548–1568.
Weaver, B.L., 1991, The origin of ocean island basalt end-member compositions: Trace element and isotopic constraints: Earth and Planetary Science Letters, v. 104, p. 381–397.
Weisenberg, C.W., and Avé Lallemant, H., 1977, Permo-Triassic emplacement of the Feather River ultramafic body, northern Sierra Nevada, California: Geological Society of America abstracts with Programs, v. 9, p. 525.
White, W.M., Hofmann, A.W., and Puchelt, H., 1987, Isotope Geochemistry of Pacific Mid-Ocean Ridge Basalt: Journal of Geophysical Research., v. 92, p. 4881–4893.
Williams, H., and Smyth, W.R., 1973, Metamorphic aureoles beneath ophiolite suites and alpine peridotites: Tectonic implications with west Newfoundland examples: American Journal of Science, v. 273, p. 594–621.
Woodhead, J.D., Greenwood, P., Harmon, R.S., and Stoffers, P., 1993, Oxygen isotope evidence for recycled crust in the source of EM-type ocean island basalts: Nature, v. 362, p. 809–813.
Yogodzinski, G.M., Kay, R.W., Volynets, O.N., Koloskov, A.V., and Kay, S.M., 1995, Magnesian andesite in the western Aleutian Komandorsky region: Implications for slab melting and processes in the mantle wedge: Geological Society of American Bulletin, v. 107, p. 505–519.

Appendix. Petrographic description of the samples

High-grade tectonic blocks

CSUH-1: This is an amphibolite from directly south of the California State University East Bay Campus. The mineral assemblage is actinolite/actinolitic hornblende + epidote + albite + quartz + phengite + titanite + chlorite.

SUNOL-2038: This is an eclogite from Sunol Regional Wilderness. The mineral assemblage is hornblende + omphacite + epidote + phengite + garnet + titanite (with small rutile cores).

JS-Ecg: This is an eclogite from Junction School west of Healdsburg. Part of the block has more hornblende and is more of an amphibolite. The amphibolite part mineral assemblage is hornblende+ omphacite, whereas the eclogite block mineral assemblage is omphacite + garnet + barroisite + phengite + rutile (rimmed with titanite). Later glaucophane rims hornblende and barroisite. Ilmenite occurs early and is overgrown by rutile and titanite.

HPSZ: This is a garnet amphibolite from the Hunter's Point shear zone. The mineral assemblage consists of hornblende + garnet + (possible former plagioclase, replaced by retrograde minerals such as lawsonite) + titanite (with local rutile cores). Glaucophane rims hornblende.

F-1: This is a garnet amphibolite from Moeser Lane in El Cerrito. The mineral assemblage is garnet + hornblende + albite + quartz + rutile. Albite and quartz are unusually abundant here suggesting this may have a more felsic protolith than the average high-grade metabasaltic block.

F-4: This is a garnet blueschist from Jenner on the north bank of the Russian River. The mineral assemblage is glaucophane + garnet + epidote + white mica. Some relict omphacite is present as inclusions in garnet, and rutile is also present as cores in titanite. This is an eclogite that retrograded to a blueschist.

F-6: This is an omphacite garnet amphibolite from Shamrock Quarry, near Laytonville. The mineral assemblage is garnet + omphacite + epidote + white mica + barroisite + rutile. As this rock contains a lot more calcic amphibole than omphacite, it is best classified as an amphibolite rather than an eclogite.

F-8: This is an eclogite from Jenner. The mineral assemblage is garnet + omphacite + barroisite + epidote + rutile (rimmed by titanite) with some late glaucophane and chlorite.

F-10: This is a blueschist from Mill Creek Road, west of Healdsburg. The mineral assemblage is glaucophane + white mica + lawsonite + chlorite + omphacite.

F-11: This is an eclogite from Mill Creek Road. The mineral assemblage is omphacite + garnet + actinolite + epidote with some late chlorite.

MP-1: This is an amphibolite block from McLaren Park in San Francisco. The mineral assemblage is hornblende + albite + epidote + titanite.

TL-4: This is an amphibolite block from Terra Linda in Marin County. The mineral assemblage is hornblende/actinolitic hornblende + albite + epidote + titanite + late actinolite.

High-grade coherent sheets

GM-1: This is a garnet amphibolite from Goat Mountain. The mineral assemblage is hornblende (brownish green) + garnet (altered to chlorite in most cases) + omphacite + white mice + rutile rimmed with titanite. There is blueschist overprint recorded by sodic amphibole rims on the hornblende.

GM-2: This is a garnet amphibolite from Goat Mountain. The mineral assemblage is hornblende (brownish green) + garnet (altered to chlorite in most cases) + omphacite + white mice + rutile rimmed with titanite. There is blueschist overprint recorded by sodic amphibole rims on the hornblende.

GM-3: This is a garnet amphibolite from Goat Mountain. The mineral assemblage is hornblende (brownish green) + garnet (altered to chlorite in most cases) + omphacite + white mice + rutile rimmed with titanite. There is blueschist overprint recorded by sodic amphibole rims on the hornblende.

F-3: This is a garnet amphibolite from the Antelope Creek Slab, Panoche Pass area. The mineral assemblage is hornblende + garnet + albite (formerly more calcic plagioclase?) + lawsonite and late glaucophane.

WC-SSS-1: This is an epidote blueschist from Ward Creek near a contact with the Skaggs Spring schist metasedimentary unit. The mineral assemblage is glaucophane + epidote + phengite + quartz + titanite + late lawsonite.

WC-MV-1: This is an epidote blueschist, Ward Creek. The mineral assemblage is glaucophane + epidote + omphacite + phengite + late lawsonite + titanite.

WC-MV-2: This is an epidote blueschist from Ward Creek. This mineral assemblage is glaucophane + epidote + omphacite + phengite + titanite + late lawsonite.

95-DIAB-14: This is a lawsonite blueschist from Willow Spring Slab, Panoche Pass area. The mineral assemblage is glaucophane + lawsonite (with epidote cores) + phengite + minor quartz + titanite.

95-DIAB-29: This is a lawsonite blueschist from Willow Spring Slab, Panoche Pass area. The mineral assemblage is glaucophane + lawsonite + phengite + pumpellyite + carbonate + titanite (some rutile cores).

95-DIAB-031: This is a fine-grained eclogite from Willow Spring Slab, Panoche Pass area. The mineral assemblage is omphacite + garnet + epidote + titanite + rare phengite + late lawsonite + late chlorite.

95-DIAB-107C: This is an eclogite from Willow Spring Slab, Panoche Pass area. The mineral assemblage is omphacite + garnet + barroisite + epidote + rutile (mostly replaced by titanite) + late sodic amphibole.

Low-grade coherent

NR-GABB: This is a gabbro from Nicasio Reservoir consisting of altered plagioclase and igneous orthopyroxene and clinopyroxene. Metamorphic minerals include pumpellyite and chlorite.

NR-PB: This is pillow basalt (vesicular) from Nicasio Reservoir. The primary igneous minerals are plagioclase and clinopyroxene. Pumpellyite occurs abundantly as veins and vesicular fillings.

MHPB: This is fairly glassy pillow basalt from Marine Headlands. Glass and plagioclase have been completely replaced by fine-grained metamorphic minerals such as pumpellyite and chlorite. There are some veins of quartz and albite.

PAC-1: This is basalt from Pacifica. This may have been a submarine tuff and was originally very glassy. Some small (igneous) plagioclase laths are present. Glass is altered to a fine-grained pumpellyite and chlorite.

SFM-1: This is an epidote blueschist of the South Fork Mountain schist from Tomhead Mountain. The mineral assemblage is glaucophane + epidote + chlorite + albite + quartz.

SFM-6: This is an epidote blueschist of the South Fork Mountain schist from Tomhead Mountain. The mineral assemblage is glaucophane + epidote + albite + quartz + chlorite.

F-9: This is a fine-grained epidote blueschist of the South Fork Mountain schist from Thomes Creek Road. The mineral assemblage is actinolite + glaucophane + epidote with some late chlorite.

F-12: This is an epidote blueschist of the South Fork Mountain schist from Thomes Creek Road. The mineral assemblage is glaucophane + epidote + actinolite + large relict igneous augite some of which are partially replaced by metamorphic acmitic clinopyroxene + quartz + albite + chlorite.

Coast Range ophiolite

MT.DIAB-1: This is basalt from Mt Diablo. There is very little noticeable metamorphism in this rock. Original igneous minerals are plagioclase laths with interstitial clinopyroxene. There is some secondary carbonate. Glass has been altered to chlorite.

HW-GABB: This is gabbro from Hayward consisting of very fresh unaltered plagioclase and pyroxene. Clinopyroxene predominates over orthopyroxene.

Feather River ultramafic belt

YR 44: This is amphibolite with hornblende + plagioclase (altered) ± clinopyroxene. This includes late actinolite and chlorite.

YR 45: This is amphibolite with hornblende + plagioclase + titanite (rutile cores) ± ilmenite. Late prenite veins are present.

FR 92-4: This is garnet amphibolite with hornblende + garnet ± epidote ± albite ± quartz + rutile.